相関電子系超伝導の多様性(I)

Diversity of Correlated Superconductivity (I)

- 重い電子系 (Heavy-electrons systems)
- 有機伝導系 (Organic Systems)
- 銅酸化物系 (Copper Oxides systems)
- 鉄ニクタイド系 (Iron Pnictides systems)
- 最近の話題

強相関電子系のモデルハミルトニアン

① ハバードハミルトニアン

$$\mathcal{H} = -t \sum_{ij\sigma} c^{\dagger}_{i\sigma} c_{j\sigma} + U \sum_{i} n_{i\uparrow} n_{i\downarrow}$$

② $t-J$ ハミルトニアン

$$\mathcal{H} = -\tilde{t} \sum_{ij\sigma} c^{\dagger}_{i\sigma} c_{j\sigma} + J \sum_{ij} \boldsymbol{S}_i \cdot \boldsymbol{S}_j$$

③ 重い電子系ハミルトニアン

$$\mathcal{H} = \sum_{k\sigma} \epsilon_k a^{\dagger}_{k\sigma} a_{k\sigma} + J_{\mathrm{K}} \sum_{l} \boldsymbol{S}_l \cdot \vec{\sigma}^{c}_{l} + J_{\mathrm{RKKY}}(R_{ij}) \sum_{ij} \boldsymbol{S}_i \cdot \boldsymbol{S}_j$$

Correlation Effect in Condensed Matter

Simple Metal $t \gg U$

Ferromagnetic (FM) Metal $t \geq U$

Metal-Insulator transition $t < U$

Antiferromagnetic Mott Insulator $t \ll U$

$$\mathcal{H} = -t \sum_{ij\sigma} c^{\dagger}_{i\sigma} c_{j\sigma} + U \sum_{i} n_{i\uparrow} n_{i\downarrow}$$

$H = 2J \Sigma_{ij} S_i \cdot S_j$

$J > 0$

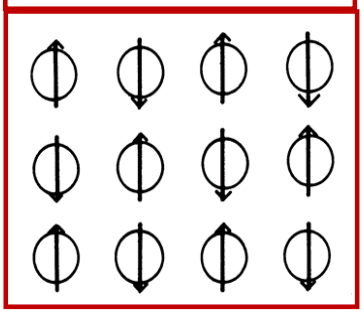

Ferromagneti
Fe (bcc)
T_c=1053 K

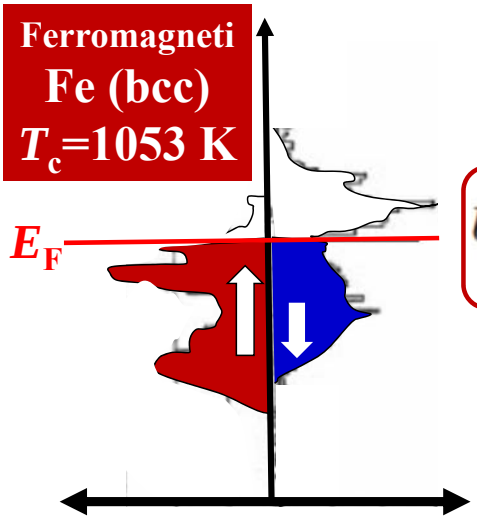

Spin Density of States

$s_{iz} = (1/2)(n_{i\uparrow} - n_{i\downarrow})$

$$U \sum_{i} n_{i,\uparrow} n_{i,\downarrow} = -2U \sum_{i} s^2_{iz}$$

Mother Compounds High-T_c Copper Oxides

Correlated Electronic State in Dimer Organic Systems

$U_{eff} \sim 2|t_L|$: Intermediate Correlation Regime

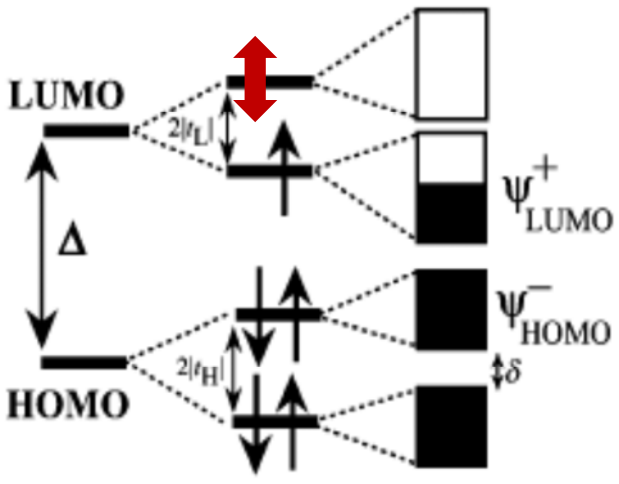

(a) Weak dimerization

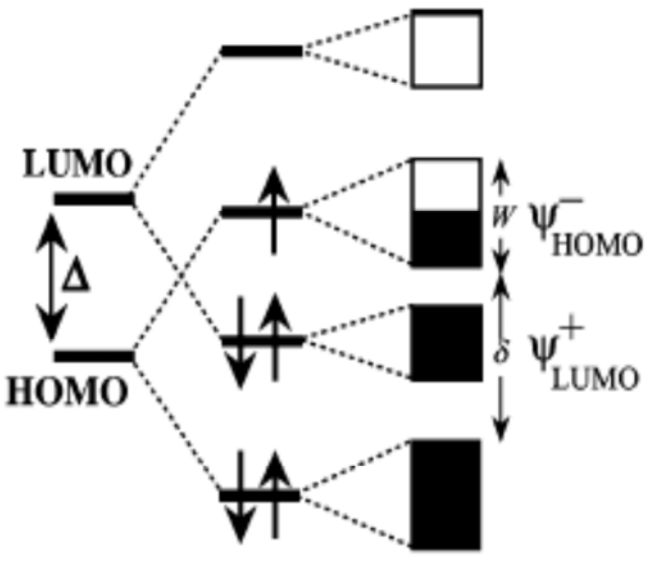

(b) Strong dimerization

$Pd(dmit)_2$ is an electron acceptor and gives salts $A[Pd(dmit)_2]_2$ with monovalent cation, A^{+1}.

有機化合物超伝導体

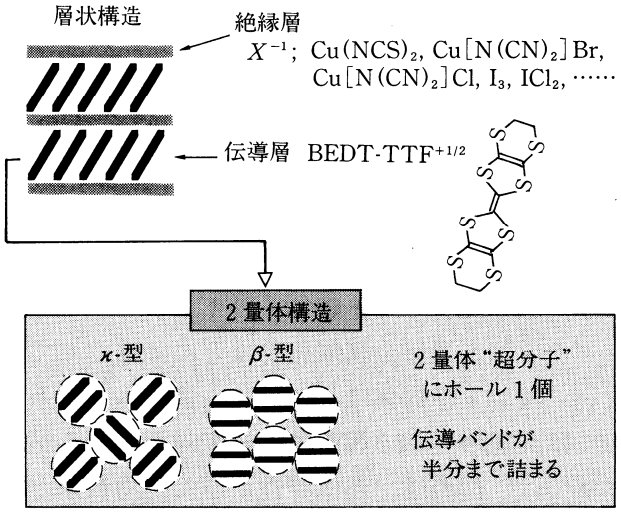

第 1 図 (BEDT-TTF)$_2X$ の構造．BEDT-TTF 分子には両側に 4 個ずつ水素が付いている．

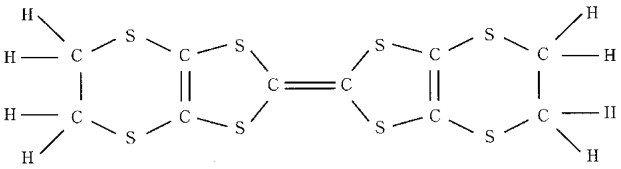

図21 (BEDT-TTF) の分子構造

超伝導ー磁性相図

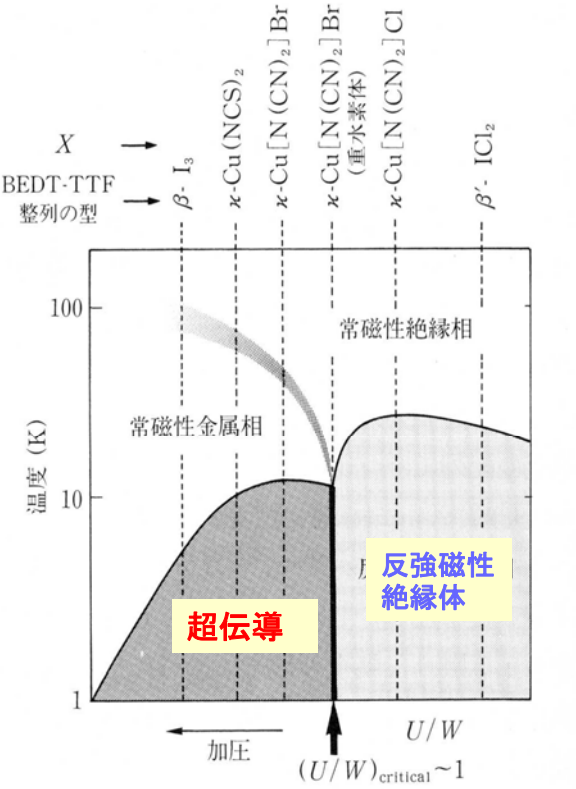

第 2 図 (BEDT-TTF)$_2X$ の超伝導相，絶縁体相を説明する概念的相図．

強相関電子系のモデルハミルトニアン

① ハバードハミルトニアン

$$\mathcal{H} = -t \sum_{ij\sigma} c_{i\sigma}^{\dagger} c_{j\sigma} + U \sum_{i} n_{i\uparrow} n_{i\downarrow}$$

② $t-J$ ハミルトニアン

$$\mathcal{H} = -\tilde{t} \sum_{ij\sigma} c_{i\sigma}^{\dagger} c_{j\sigma} + J \sum_{ij} \boldsymbol{S}_i \cdot \boldsymbol{S}_j$$

③ 重い電子系ハミルトニアン

$$\mathcal{H} = \sum_{k\sigma} \epsilon_k a_{k\sigma}^{\dagger} a_{k\sigma} + J_{\mathrm{K}} \sum_{l} \boldsymbol{S}_l \cdot \vec{\sigma}_l^{c} + J_{\mathrm{RKKY}}(R_{ij}) \sum_{ij} \boldsymbol{S}_i \cdot \boldsymbol{S}_j$$

Correlation Effect in Condensed Matter

Simple Metal $t >> U$

Ferromagnetic (FM) Metal $t \geq U$

Metal-Insulator transition $t < U$

Antiferromagnetic Mott Insulator $t << U$

$$\mathcal{H} = -t \sum_{ij\sigma} c^{\dagger}_{i\sigma} c_{j\sigma} + U \sum_{i} n_{i\uparrow} n_{i\downarrow}$$

$H = 2J \Sigma_{ij} S_i \cdot S_j$

$J > 0$

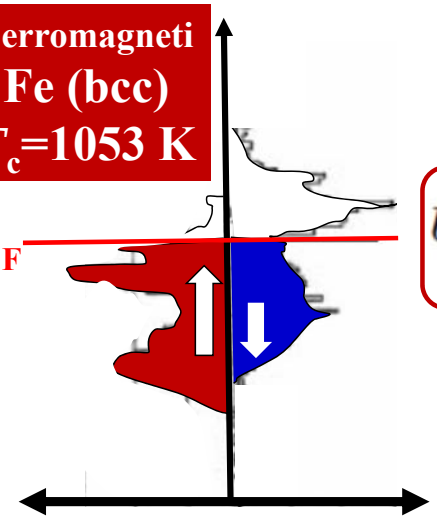

Ferromagneti
Fe (bcc)
T_c=1053 K

E_F

Spin Density of States

$s_{iz} = (1/2)(n_{i\uparrow} - n_{i\downarrow})$

$$U \sum_{i} n_{i,\uparrow} n_{i,\downarrow} = -2U \sum_{i} s^2_{iz}$$

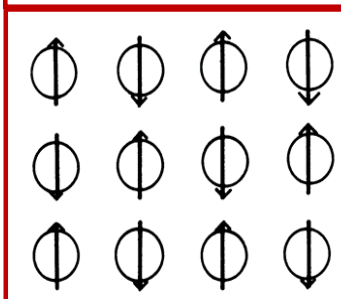

Mother Compounds High-T_c Copper Oxides

On-site Repulsive Interaction U plays vital role for emergent phases

Carrier doping into Mott insulator

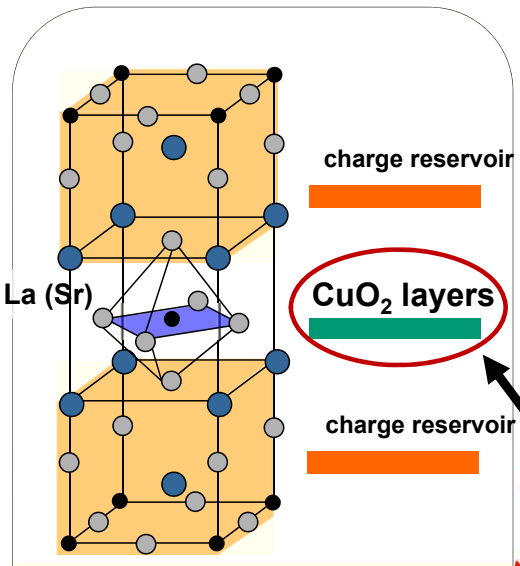

La_2CuO_4

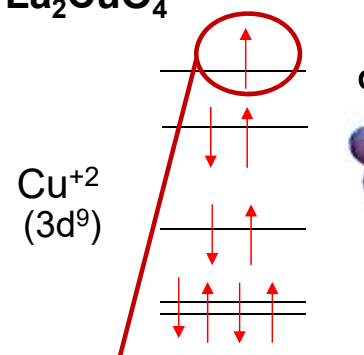

$La^{3+}_{2-x}Sr^{2+}_{x}CuO_4$

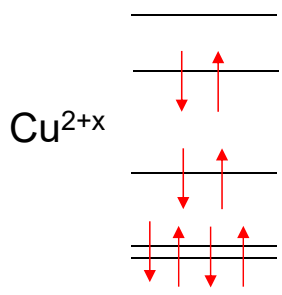

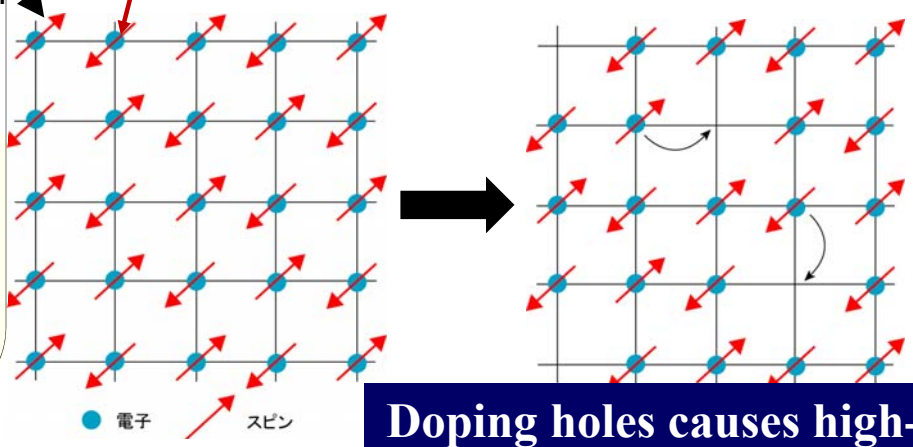

Antiferromagnetic Mott insulator

Doping holes causes high-T_c superconductivity

Novel Phase Diagram of Antiferromagnetic Order and Superconductivity in Copper Oxides

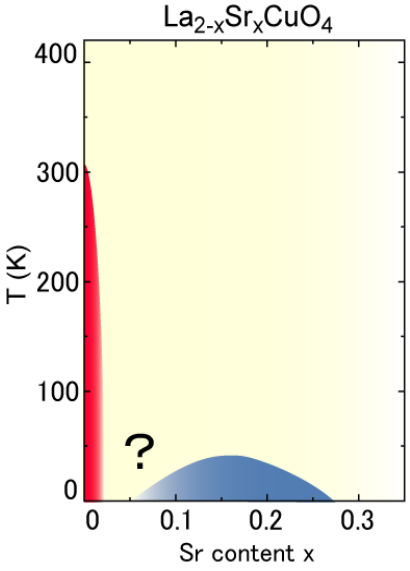

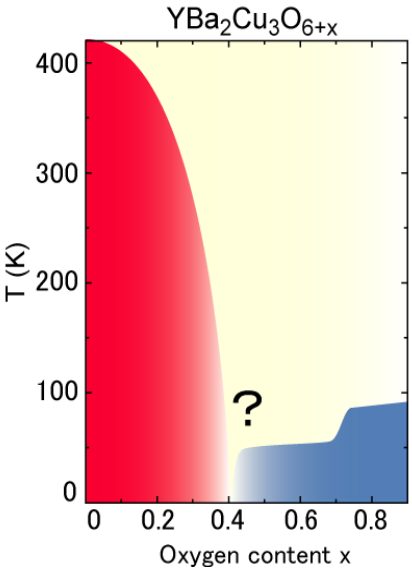

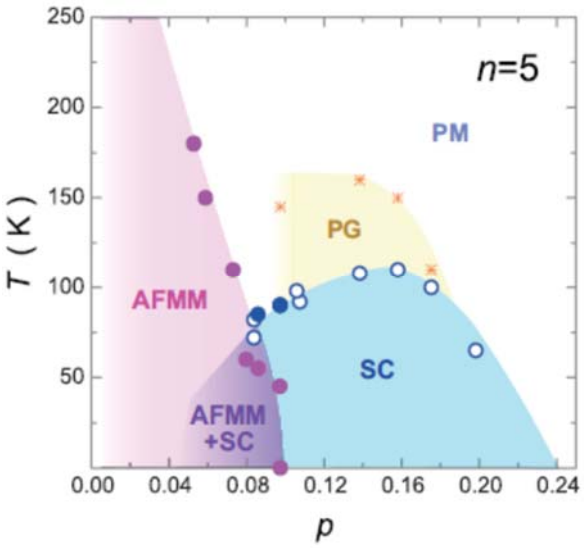

Towards understanding a concept for high-T_c cuprate

Carrier doping

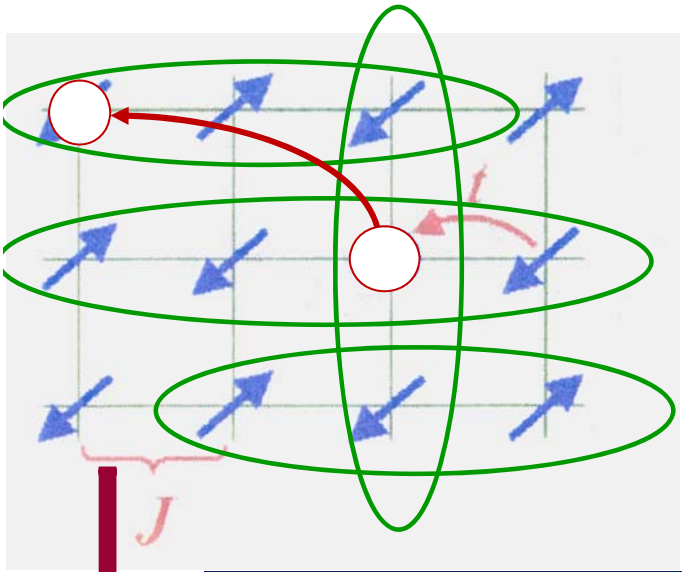

Delocalized resonating spin-singlet pairs

AFM + *d*-wave SC

$$H = \sum_{\langle i,j \rangle} t_{ij} a^{\dagger}_{i\sigma} a_{j\sigma} + \sum_{i} J_{ij} \boldsymbol{S}_i \cdot \boldsymbol{S}_j$$

Variational Monte Carlo on the t – J model

S. Pathak et al., PRL 102, 027002 (2009)

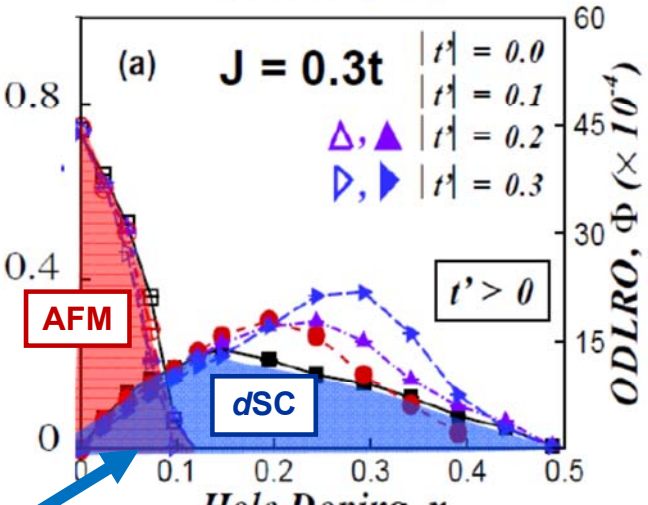

G. J. Chen et al., PRB 42, 2662 (1990).
T. Giamarchi et al., PRB 43, 12 943(1991).
A. Himeda and M. Ogata, PRB 60, R9935 (1999).
T.K. Lee and C.T. Shih, Phys. Rev. B 55 (1997) 5983.

Summary

	Copper Oxides
Mother compound	AFM-Mott Insulators ($T_N \sim 500$ K)
Phase diagram	Carrier doping
Electronic state	Single band
SC symmetry	d wave ($T_c = 135$ K)
Pairing interaction	AFM Super-exchange Interaction J

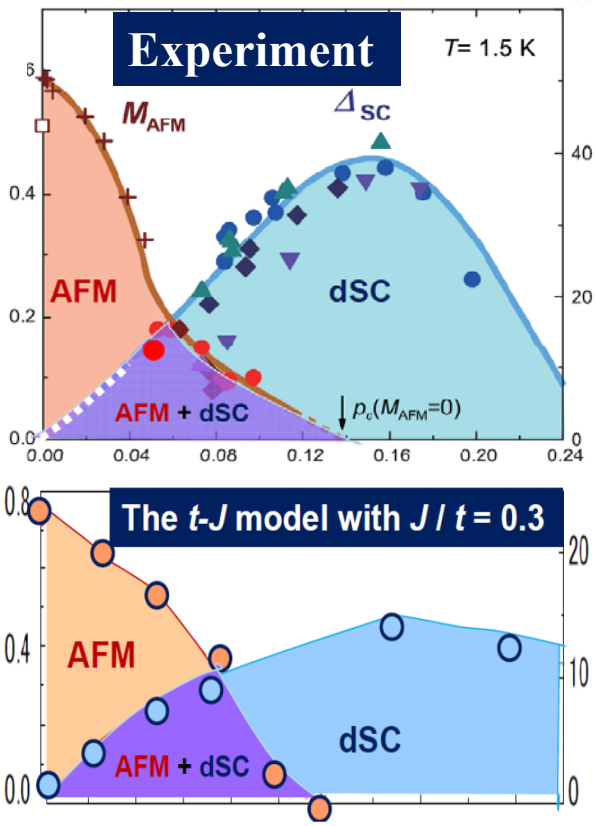

$$H = \sum_{\langle i,j \rangle} t_{ij} a^{\dagger}_{i\sigma} a_{j\sigma} + \sum_{i} J_{ij} \boldsymbol{S}_i \cdot \boldsymbol{S}_j$$

In strong coupling regime of electron correlation ($U > 8t$) :
Doped Mott Insulator is the superconductor, leading to the high T_c superconductivity mediated by the AFM super-exchage interaction!!

強相関電子系のモデルハミルトニアン

① ハバードハミルトニアン

$$\mathcal{H} = -t \sum_{ij\sigma} c^{\dagger}_{i\sigma} c_{j\sigma} + U \sum_{i} n_{i\uparrow} n_{i\downarrow}$$

② $t-J$ ハミルトニアン

$$\mathcal{H} = -\tilde{t} \sum_{ij\sigma} c^{\dagger}_{i\sigma} c_{j\sigma} + J \sum_{ij} S_i \cdot S_j$$

③ 重い電子系ハミルトニアン

$$\mathcal{H} = \sum_{k\sigma} \epsilon_k a^{\dagger}_{k\sigma} a_{k\sigma} + J_{\mathrm{K}} \sum_{l} S_l \cdot \vec{\sigma}^{c}_{l} + J_{\mathrm{RKKY}}(R_{ij}) \sum_{ij} S_i \cdot S_j$$

Heavy-electrons Compounds

RKKY interaction

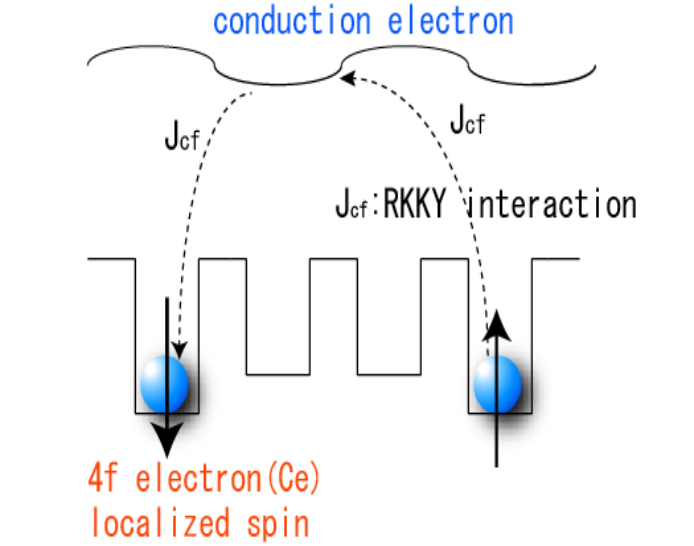

Antiferromagnetic state

Spin quenching (Kondo) effect

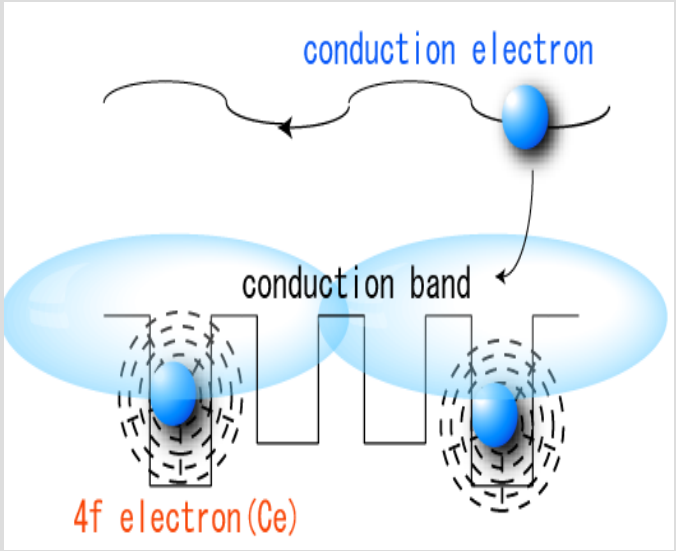

Heavy-electron liquid

Heavy-electron Superconductivity

1979 First Discovery of SC in heavy electron materials $CeCu_2Si_2$

(T_c= 0.6 K)

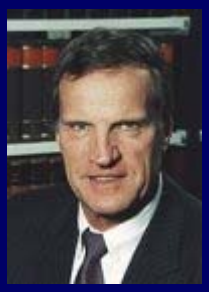

Steglich
(ドイツ)

AFM

4*f*-spin — RKKY interaction (ルダーマン-キッテル-糟谷-芳田) — 4*f*-spin

localization ⟷ itinerant

Kondo effect
(近藤 淳)

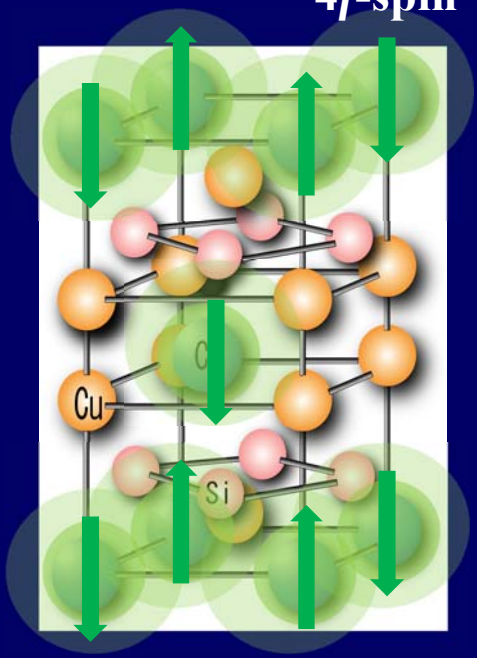

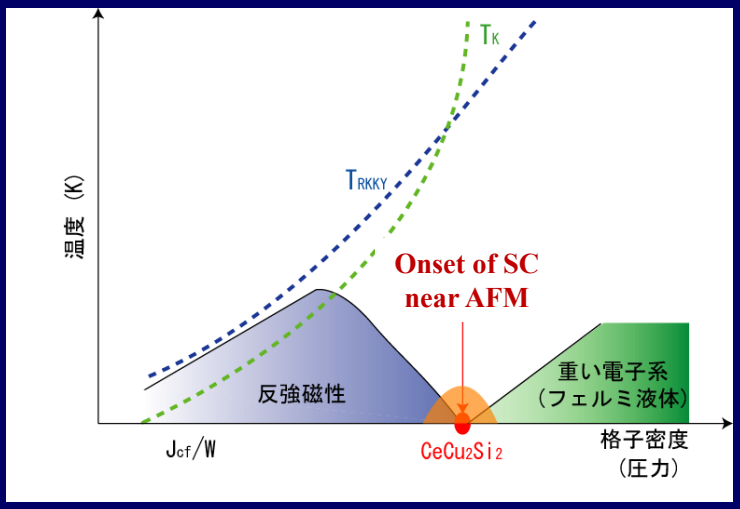

Dome type of SC phase is formed around quantum critical point for AFM

Periodic Table for atomic element

（基底状態の中性原子の外殻電子配置）

原子およびイオンの電子配置を示す記号については，すべての初歩的な原子物理学の教科書において述べられている．文字 s，p，d…は $\hbar$ を単位とする軌道角モーメント 0, 1, 2, をもっている電子を示す．文字の左側の数字は軌道の主量子数を示す．右肩上の数字

H^{1} $1s$																	He^{2} $1s^2$
Li^{3} $2s$	Be^{4} $2s^2$											B^{5} $2s^22p$	C^{6} $2s^22p^2$	N^{7} $2s^22p^3$	O^{8} $2s^22p^4$	F^{9} $2s^22p^5$	Ne^{10} $2s^22p^6$
Na^{11} $3s$	Mg^{12} $3s^2$											Al^{13} $3s^23p$	Si^{14} $3s^23p^2$	P^{15} $3s^23p^3$	S^{16} $3s^23p^4$	Cl^{17} $3s^23p^5$	Ar^{18} $3s^23p^6$
K^{19} $4s$	Ca^{20} $4s^2$	Sc^{21} $3d$ $4s^2$	Ti^{22} $3d^2$ $4s^2$	V^{23} $3d^3$ $4s^2$	Cr^{24} $3d^5$ $4s$	Mn^{25} $3d^5$ $4s^2$	Fe^{26} $3d^6$ $4s^2$	Co^{27} $3d^7$ $4s^2$	Ni^{28} $3d^8$ $4s^2$	Cu^{29} $3d^{10}$ $4s$	Zn^{30} $3d^{10}$ $4s^2$	Ga^{31} $4s^24p$	Ge^{32} $4s^24p^2$	As^{33} $4s^24p^3$	Se^{34} $4s^24p^4$	Br^{35} $4s^24p^5$	Kr^{36} $4s^24p^6$
Rb^{37} $5s$	Sr^{38} $5s^2$	Y^{39} $4d$ $5s^2$	Zr^{40} $4d^2$ $5s^2$	Nb^{41} $4d^4$ $5s$	Mo^{42} $4d^5$ $5s$	Tc^{43} $4d^6$ $5s$	Ru^{44} $4d^7$ $5s$	Rh^{45} $4d^8$ $5s$	Pd^{46} $4d^{10}$ –	Ag^{47} $4d^{10}$ $5s$	Cd^{48} $4d^{10}$ $5s^2$	In^{49} $5s^25p$	Sn^{50} $5s^25p^2$	Sb^{51} $5s^25p^3$	Te^{52} $5s^25p^4$	I^{53} $5s^25p^5$	Xe^{54} $5s^25p^6$
Cs^{55} $6s$	Ba^{56} $6s^2$	La^{57} $5d$ $6s^2$	Hf^{72} $4f^{14}$ $5d^2$ $6s^2$	Ta^{73}	W^{74}	Re^{75}	Os^{76}	Ir^{77}	Pt^{78}	Au^{79}	Hg^{80} $5d^{10}$ $6s^2$	Tl^{81} $6s^26p$	Pb^{82} $6s^26p^2$	Bi^{83} $6s^26p^3$	Po^{84} $6s^26p^4$	At^{85} $6s^26p^5$	Rn^{86} $6s^26p^6$
Fr^{87} $7s$	Ra^{88} $7s^2$	Ac^{89} $6d$ $7s^2$															

Ce^{58} $4f^2$ $6s^2$	Pr^{59} $4f^3$ $6s^2$	Nd^{60} $4f^4$ $6s^2$	Pm^{61} $4f^5$ $6s^2$	Sm^{62} $4f^6$ $6s^2$	Eu^{63} $4f^7$ $6s^2$	Gd^{64} $4f^7$ $5d$ $6s^2$	Tb^{65} $4f^8$ $5d$ $6s^2$	Dy^{66} $4f^{10}$ $6s^2$	Ho^{67} $4f^{11}$ $6s^2$	Er^{68} $4f^{12}$ $6s^2$	Tm^{69} $4f^{13}$ $6s^2$	Yb^{70} $4f^{14}$ $6s^2$	Lu^{71} $4f^{14}$ $5d$ $6s^2$
Th^{90} – $6d^2$ $7s^2$	Pa^{91} $5f^2$ $6d$ $7s^2$	U^{92} $5f^3$ $6d$ $7s^2$	Np^{93} $5f^4$ $7s^2$	Pu^{94} $5f^6$ $7s^2$	Am^{95} $5f^7$ $7s^2$	Cm^{96} $5f^7$ $6d$ $7s^2$	Bk^{97}	Cf^{98}	Es^{99}	Fm^{100}	Md^{101}	No^{102}	Lr^{103}

3d Transition elements

4f Rare earth elements

Effective atomic potentials for Ce and U

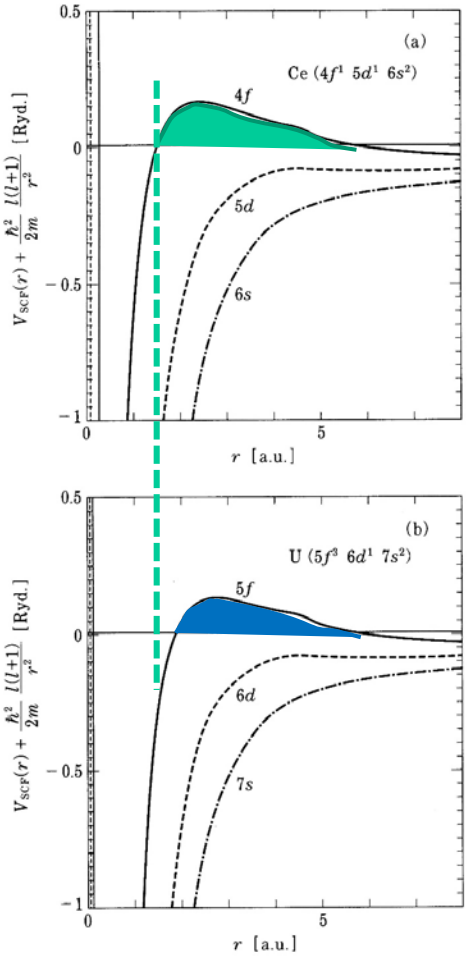

$$\left[-\frac{d^2}{dr^2}-\frac{2}{r}\frac{d}{dr}+U(r)+\frac{l(l+1)}{r^2}\right]\phi=k^2\phi,$$

$$U(r)=\frac{2m}{\hbar^2}V(r),$$

$$\varepsilon=\frac{\hbar^2k^2}{2m}.$$

Anderson Hamiltonian in Strongly Correlated systems

$$\mathcal{H} = \sum_k \sum_\sigma \varepsilon_k c^\dagger_{k\sigma} c_{k\sigma} + \sum_\sigma E_f f^\dagger_\sigma f_\sigma + U n_{f\uparrow} n_{f\downarrow}$$

$$+ \frac{1}{\sqrt{N_0}} \sum_k \sum_\sigma \left(V_{fk} f^\dagger_\sigma c_{k\sigma} + V_{kf} c^\dagger_{k\sigma} f_\sigma \right)$$

Ce: $4f^1$, $5d^1$, $6s^2$

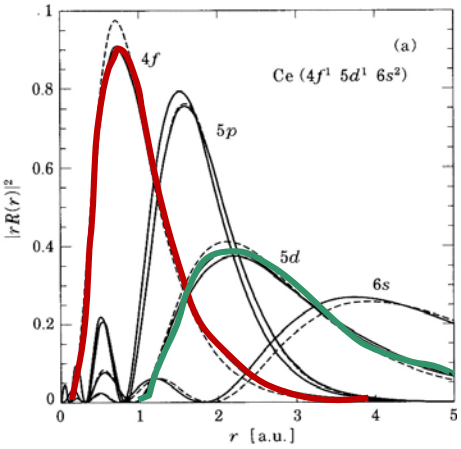

Radial distributions of wave functions of Ce and U

Hybridization term in Anderson Hamiltonian

$$\left\langle \frac{1}{\sqrt{\Omega}} e^{i\boldsymbol{k}\cdot\boldsymbol{r}} \middle| H \middle| u_{k_0} Y_{lm} \right\rangle$$

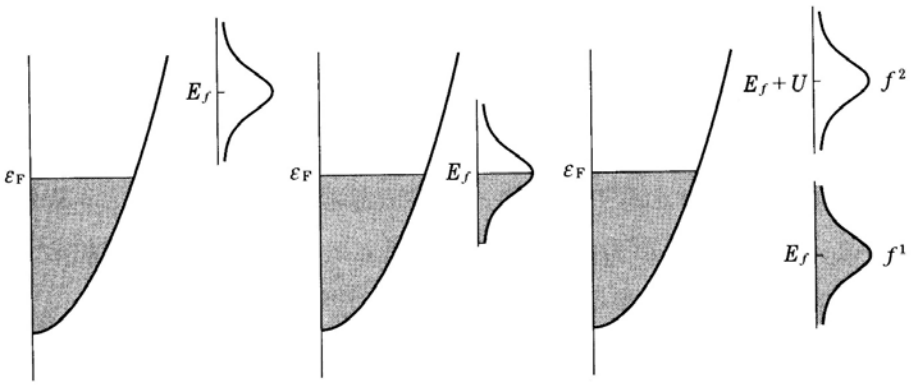

(a) $E_f - \varepsilon_F \gg \Delta$　(b) 価数揺動レジーム　(c) 近藤レジーム

Magnetic state of Ce^{3+} ($4f^1$) and U^{4+} ($5f^2$)

$4f^1$: $S = 1/2$, $L = 3$, $J = 3\text{-}1/2 = 5/2$

$5f^2$: $S = 1$, $L = 5$, $J = 5\text{-}1 = 4$

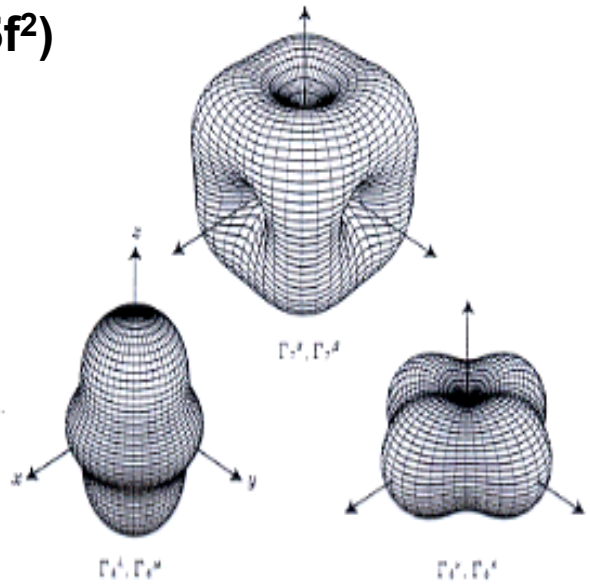

2-6図 Ce^{3+} イオンの立方晶での空間電荷分布

		Spin-Orbit	Crystal Field
Ce 化合物	Ce^{3+} ($4f^1$)	$J = \frac{5}{2}$	$\Gamma = \frac{1}{2}$
U 化合物	U^{4+} ($5f^2$)	$J = 4$	hybridization $S = \frac{1}{2}$?

Cubic crystal field effect for $J = 5/2$ ⟹

$$|\Gamma_8^v\rangle = \sqrt{\frac{5}{6}}\left|\frac{5}{2}\right\rangle + \frac{1}{\sqrt{6}}\left|-\frac{3}{2}\right\rangle$$

$$|\Gamma_8^c\rangle = \sqrt{\frac{5}{6}}\left|-\frac{5}{2}\right\rangle + \frac{1}{\sqrt{6}}\left|\frac{3}{2}\right\rangle$$

$$|\Gamma_7^+\rangle = \left|\frac{1}{2}\right\rangle$$

$$|\Gamma_7^-\rangle = \left|-\frac{1}{2}\right\rangle$$

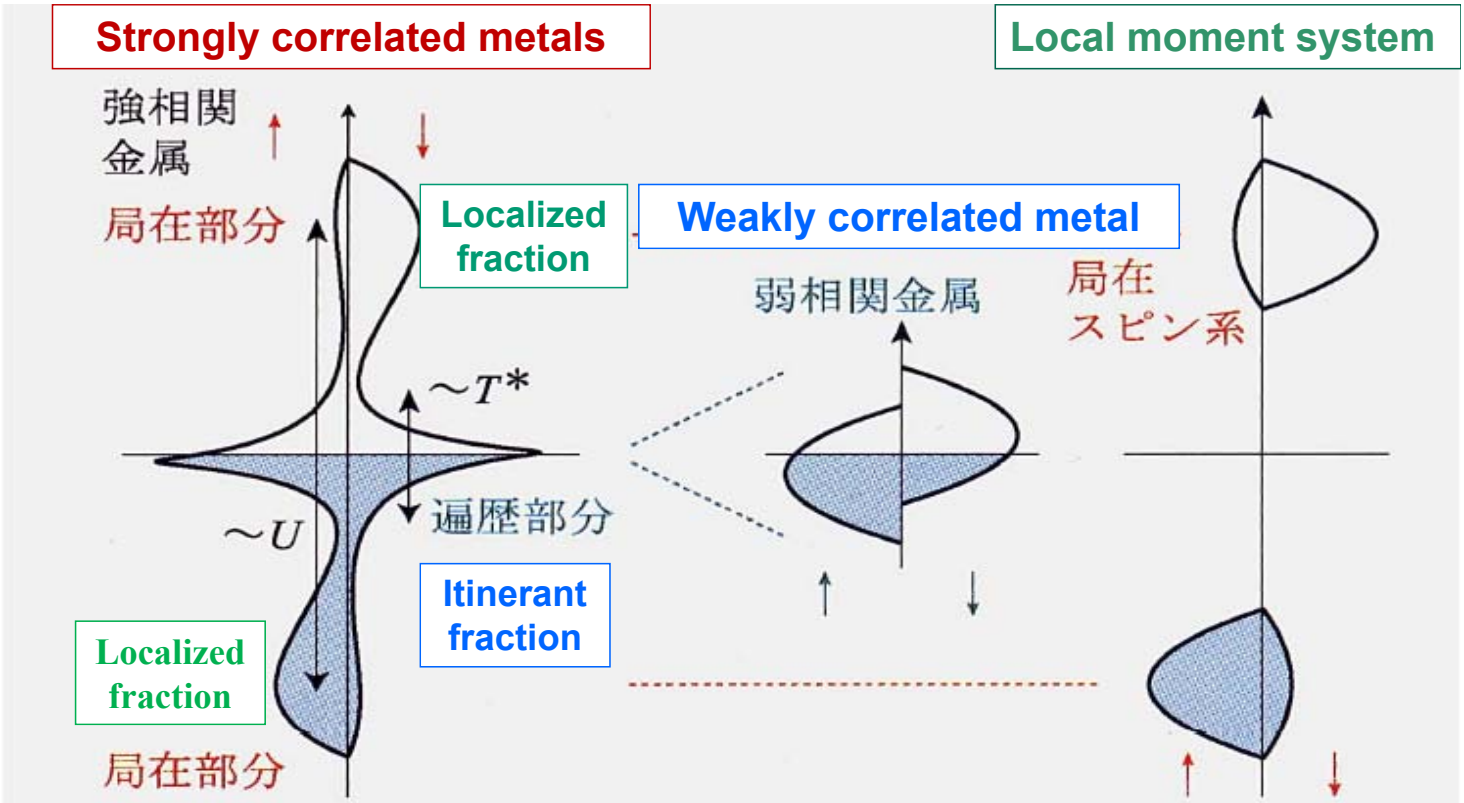

第 2 図
反強磁性状態における強相関金属の遍歴・局在二重性．弱相関金属・局在スピン系との状態密度による対比（A サイト，$T \ll T^*$）．

$$\mathcal{H} = \sum_{k\sigma} \varepsilon_k a^\dagger_{k\sigma} a_{k\sigma} + J_K \sum_i \vec{\sigma} \cdot \vec{S}_i + J_{RKKY} \sum_{\langle ij \rangle} \vec{S}_i \cdot \vec{S}_j$$

$J_K \sim |V|^2/U$　　$U \to$ large (Coulomb repulsion)

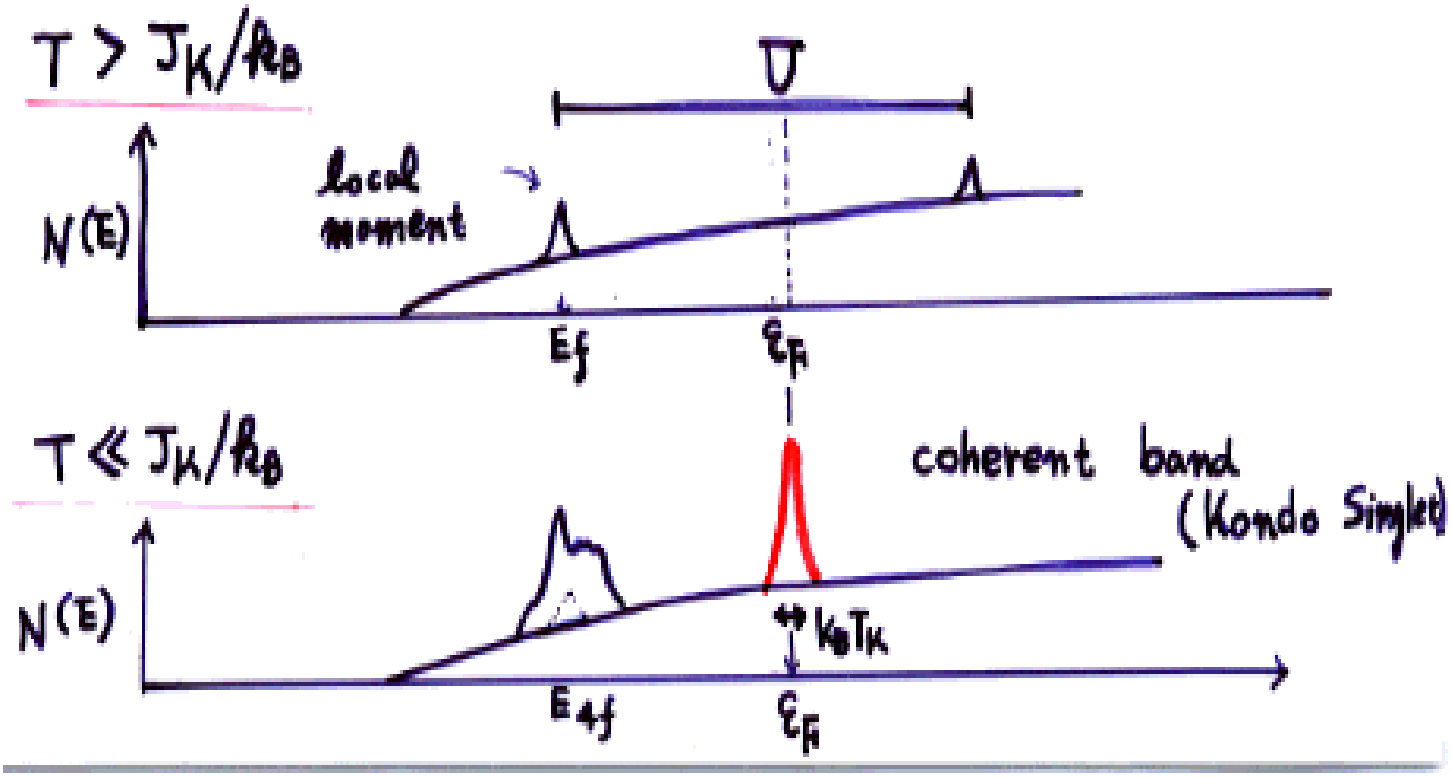

Characteristic Energy Scales in Heavy- electrons Systems

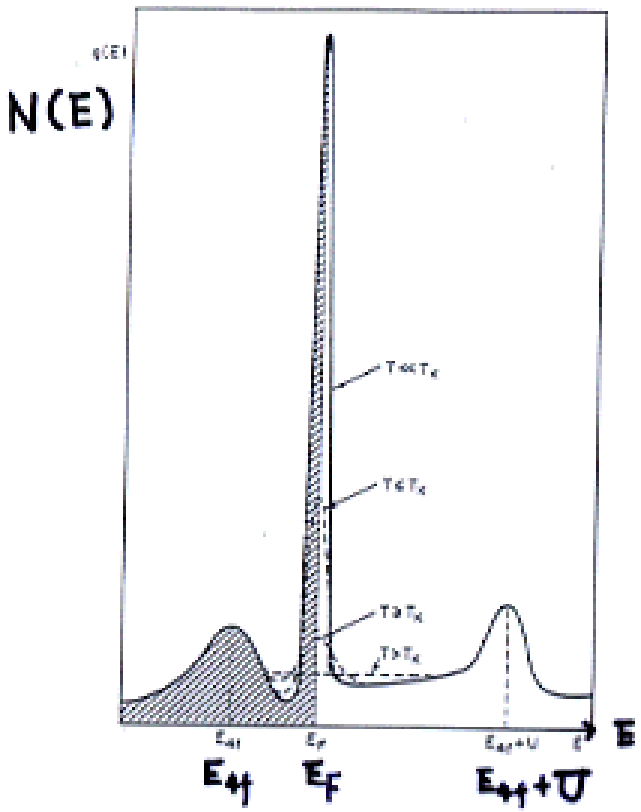

$$J_K \simeq \frac{V_{sf}^2}{E_F - E_{4f}} \sim 1 - 10meV$$

$$T_K \simeq T_F \exp\left[-\frac{1}{N_c(E_F)J_K}\right] \sim 10 - 100K$$

$$J_{RKKY} \simeq \frac{J_K^2}{E_F}$$

$$N(E_F) = \frac{3N_A}{\hbar^2 k_F^2} \cdot m^*$$

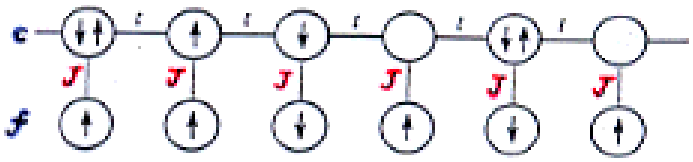

Experimental evidences for heavy electrons

- Specific Heat

$$C = \frac{\pi^2 k_B^2}{3} \rho(E_F) \cdot T = \gamma T$$

Ce, U Compounds

$\gamma \approx 1000 mJ/mole\,K^2$

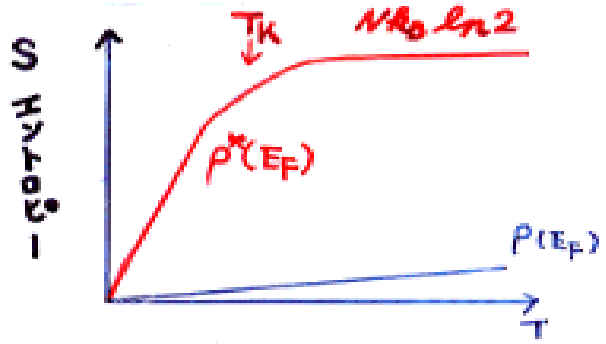

Free Electron

$\gamma_0 \simeq 1 mJ/mole \cdot K^2$

- Susceptibility

$$\chi = \mu_B^2 \rho(E_F)$$

$\chi = (1 \sim 5) \times 10^{-2}$ emu/mole

$F = E - TS$, S:Entropy

F:Free energy

$\chi_0 = 1.2 \times 10^{-5}$ emu/moleK^2

$$\rho(E_F) = \frac{3N}{2E_F} = \frac{3N}{\hbar^2 k_F^2} m$$

$m^* \approx 1000 m_0$ ← 重い電子系 Heavy Electron

Magnetic and transport behaviors in various Ce ($4f^1$) compounds

Magnetic susceptibility

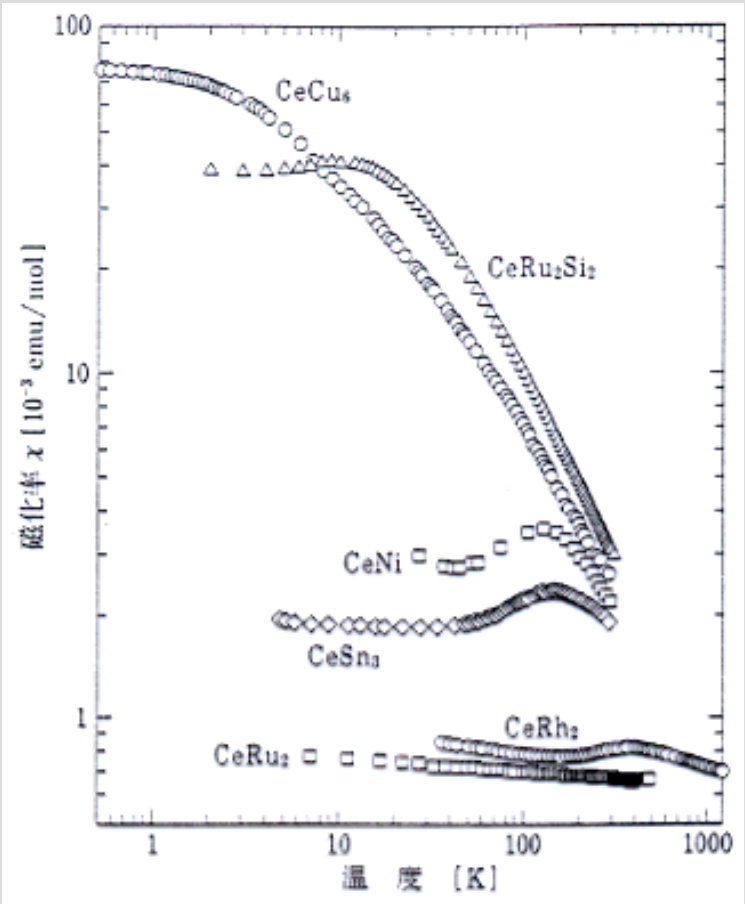

Resistance

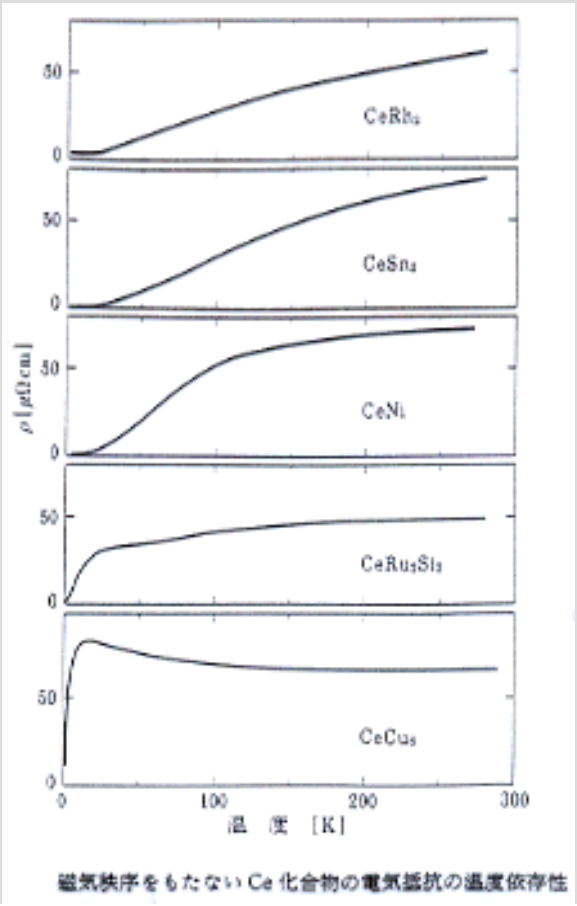

磁気秩序をもたない Ce 化合物の電気抵抗の温度依存性

$(1/T_1T) \propto N^*(E_F)^2$

Coherence effect in resistivity $\rho(T)$ due to Ce periodic lattice

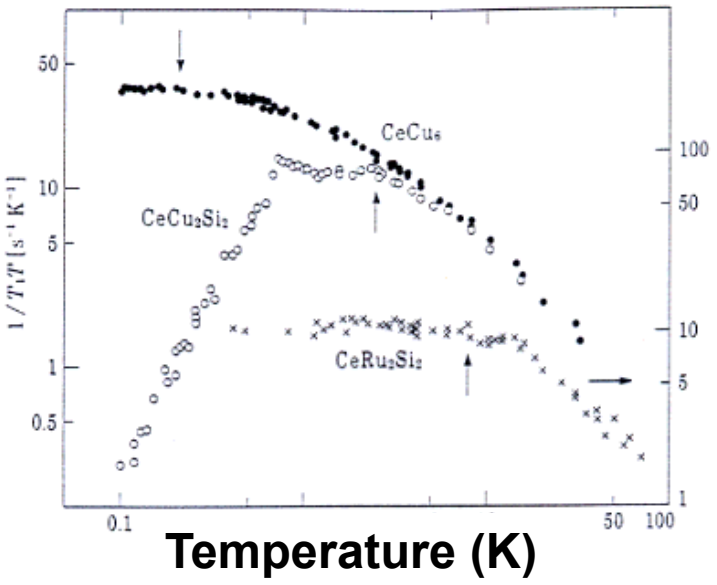

6 - 12 図　$CeCu_6$, $CeCu_2Si_2$, $CeRu_2Si_2$ の $(T_1T)^{-1}$ の温度依存性（Y

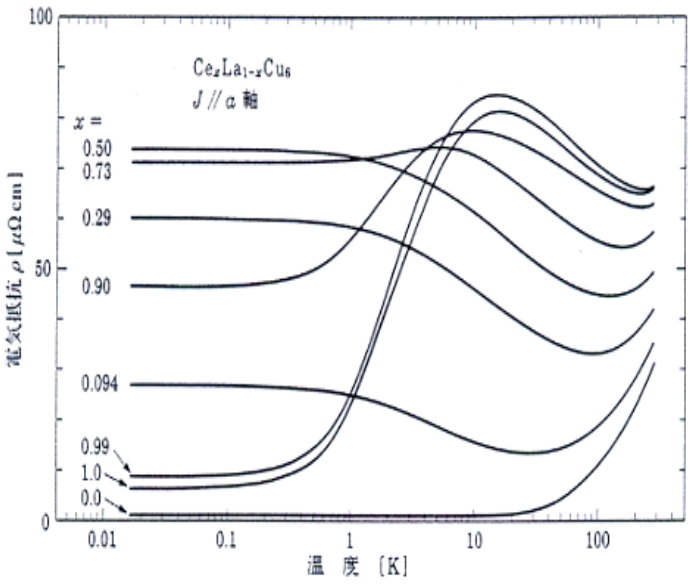

Signature of Heavy Effective Mass

Resistivity 電気抵抗

"Kondo Lattice"

"log T" → "Kondo effect"

ρ μΩ·cm

$\rho = \rho_0 + AT^2$

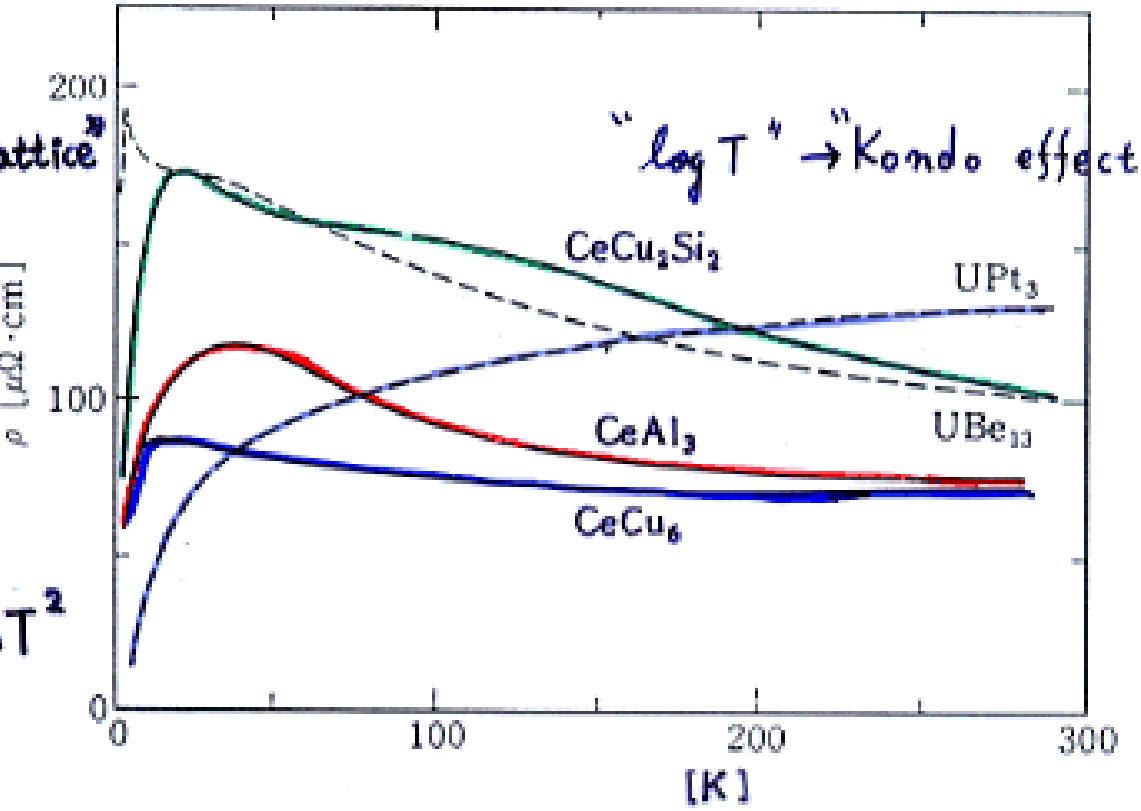

$A \propto \gamma^2$

Specific Heat 比熱

$C = \gamma T$

電子比熱係数

$\frac{C}{T}$

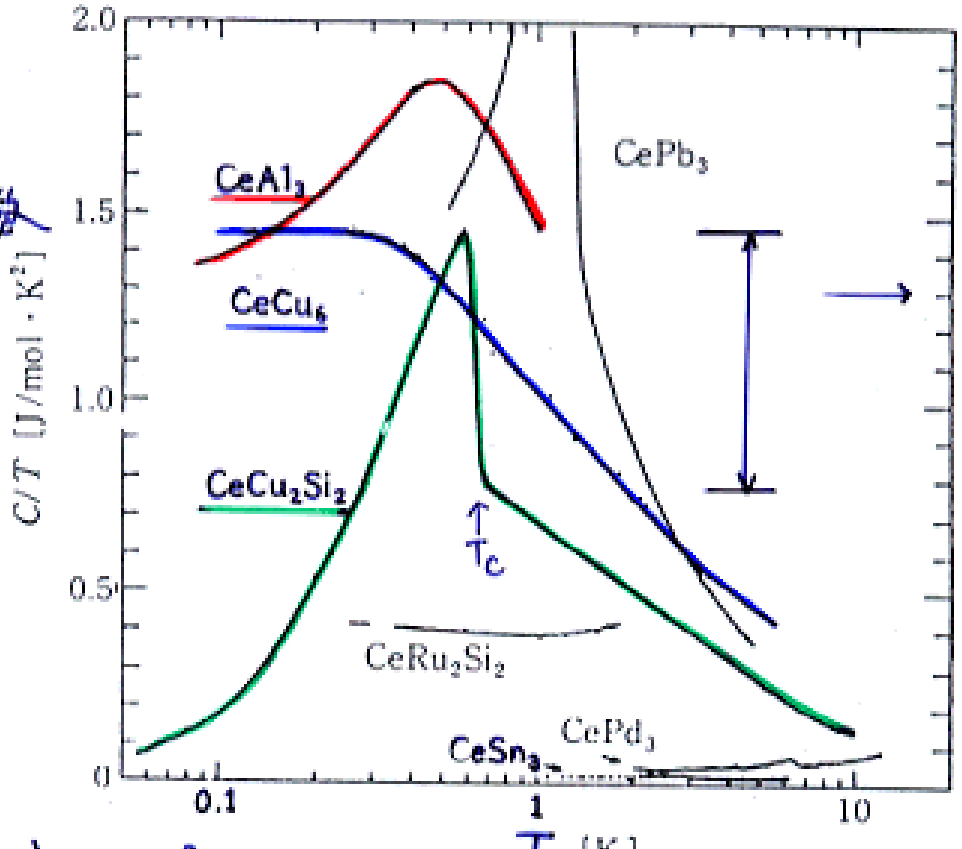

$\frac{\Delta C}{\gamma T_c} \simeq 1.2$

$C/T = \gamma_e + \beta T^2 + \cdots$

1979 Steglich et al.

	T_c(K)	crystal structure	nucleus	$1/T_1$	K^*	parity	symmetry
$CeCu_2Si_2$[17,22–25]	~ 0.7 K	tetragonal($ThCr_2Si_2$)	Cu, Si[26,27]	T^3	decrease	even	d
$CeCoIn_5$[20,21]	~ 2.3 K	tetragonal($HoCoGa_5$)	Co, In[28]	T^3	decrease	even	d
$CeIrIn_5$[20,21]	~ 0.4 K	tetragonal($HoCoGa_5$)	In[29]	T^3	-	-	-
UBe_{13}[18,19]	~ 0.9 K	cubic($NaZn_{13}$)	Be[30]	T^3	-	-	-
UPt_3[18,19]	~ 0.55 K	hexagonal	Pt[31–34]	T^3	unchange	odd	f
URu_2Si_2[18,19]	~ 1.2 K	tetragonal($ThCr_2Si_2$)	Ru, Si[35,36]	T^3	unchange	odd	
UNi_2Al_3[18,19]	~ 1 K	hexagonal	Al[37]	T^3	unchange	odd	p or f
UPd_2Al_3[18,19]	~ 2 K	hexagonal	Pd, Al[38,39]	T^3	decrease	even	d
$CeCu_2Ge_2$[40]	~ 0.6 K ($P \sim 7.6$ GPa)	tetragonal($ThCr_2Si_2$)	-	-	-	-	-
$CeIn_3$[41–45]	~ 0.2 K ($P \sim 2.5$ GPa)	cubic($AuCu_3$)	In[46]	T^3	-	-	-
$CePd_2Si_2$[41,42,47]	~ 0.4 K ($P \sim 2.5$ GPa)	tetragonal($ThCr_2Si_2$)	-	-	-	-	-
$CeRh_2Si_2$[48,49]	~ 0.2 K ($P \sim 1.0$ GPa)	tetragonal($ThCr_2Si_2$)	-	-	-	-	-
$CeRhIn_5$[50,51]	~ 2.1 K ($P \sim 1.6$ GPa)	tetragonal($HoCoGa_5$)	In[52,53]	T^3	-	-	-
High-T_c cuprates	~ 140 K (max)	perovskite	Cu, O	T^3	decrease	even	d
Sr_2RuO_4[54,55]	~ 1.5 K	perovskite	Ru, O	T^3	unchange	odd	p

Table I. Superconducting characteristics in most heavy-fermion systems along with high-T_c cupper oxides and Sr_2RuO_4. Note that the nuclear relaxation rate $1/T_1$ reveals no coherence peak just below T_c, followed by the T^3 dependence without an exception. K^* denotes the spin component of Knight shift below T_c. In this context, all unconventional superconductors discovered to date possess the line-node gap on the Fermi surface regardless of either spin-singlet d wave or spin-triplet p-wave.

文献:JPSJ, 74 (2005) 186-199."Unconventional SC in HFs"

Pressure-induced phase diagrams of AFM and SC

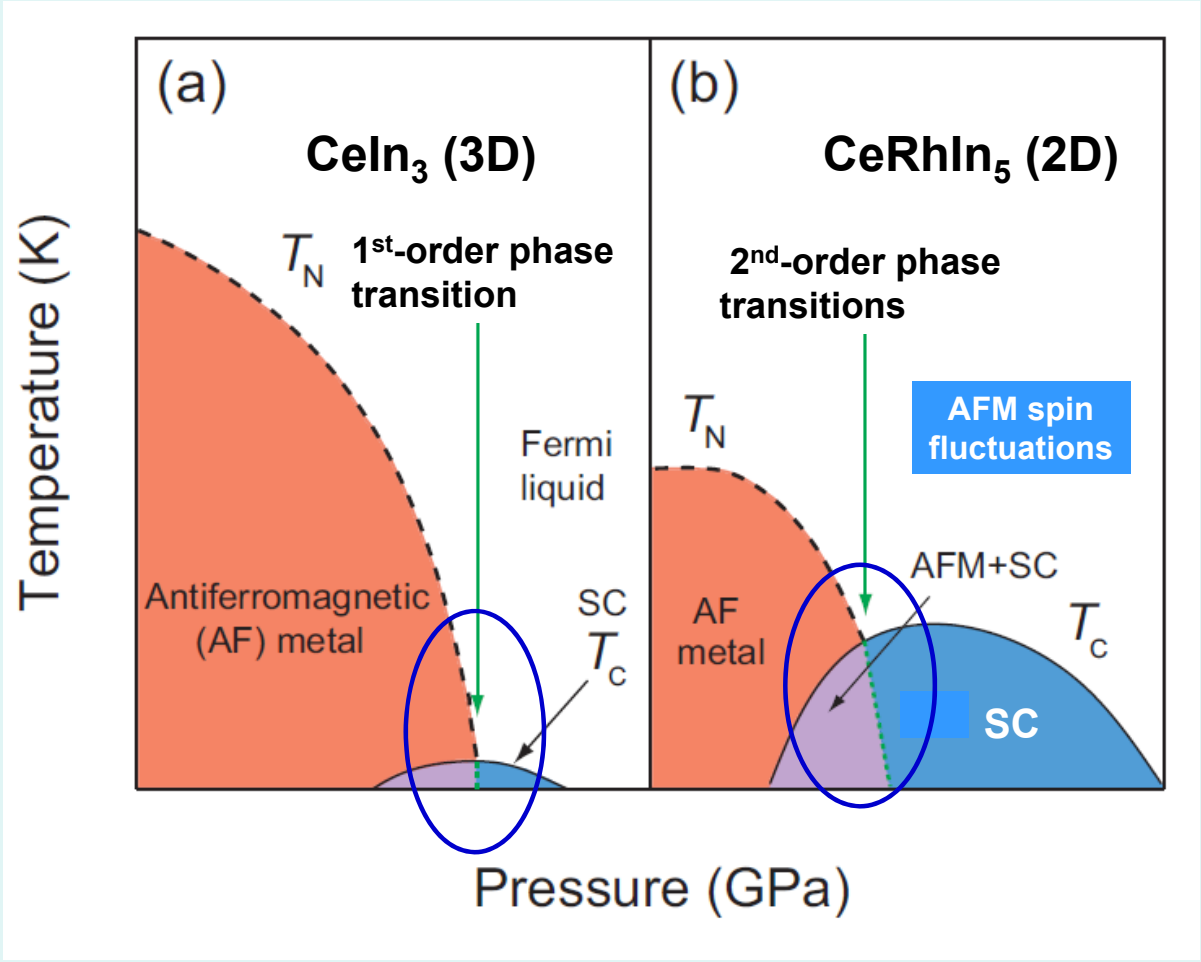

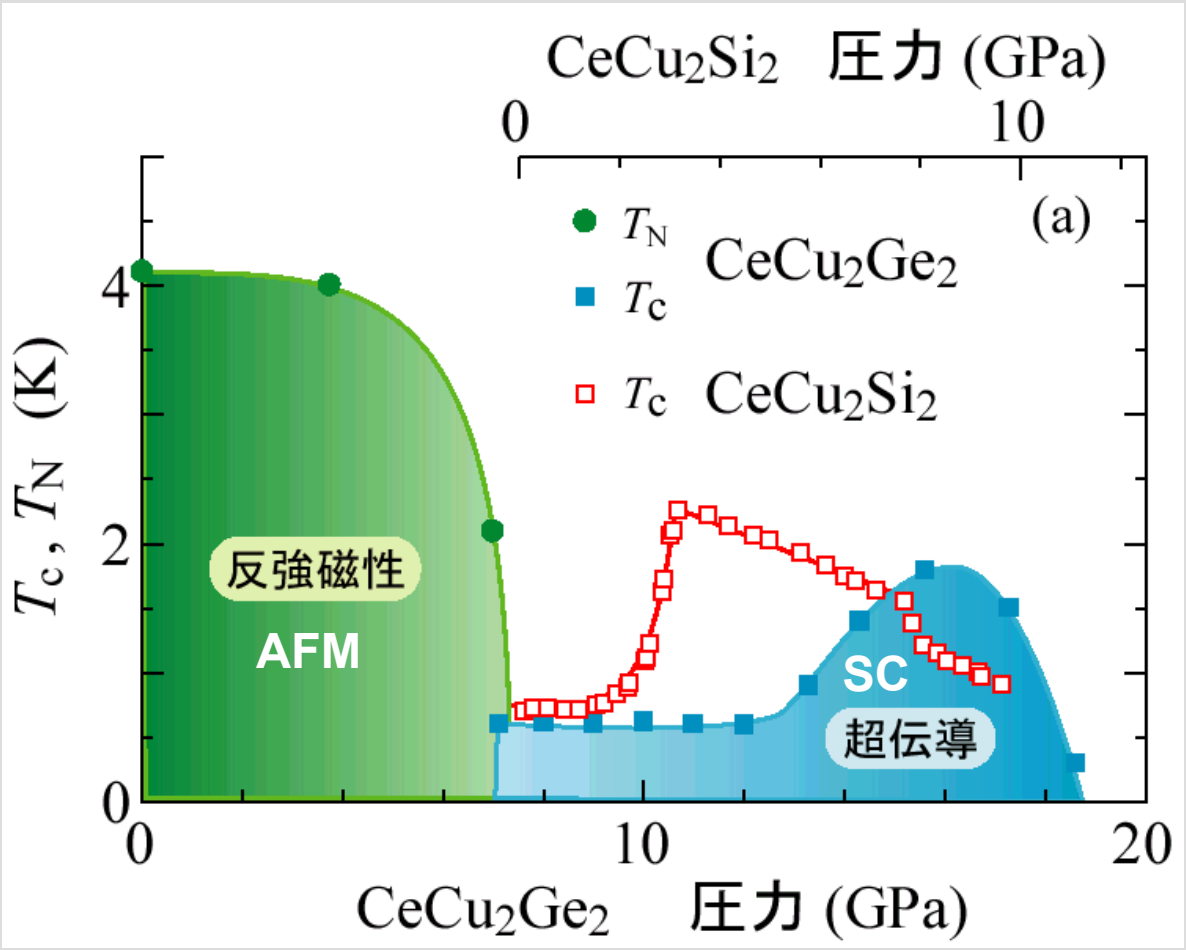
CeCu2Si2 圧力 (GPa)
0
10
(a)
TN
Tc
CeCu2Ge2
Tc
CeCu2Si2
4
2
0
Tc , TN (K)
反強磁性
AFM
SC
超伝導
0
10
20
CeCu2Ge2 圧力 (GPa)

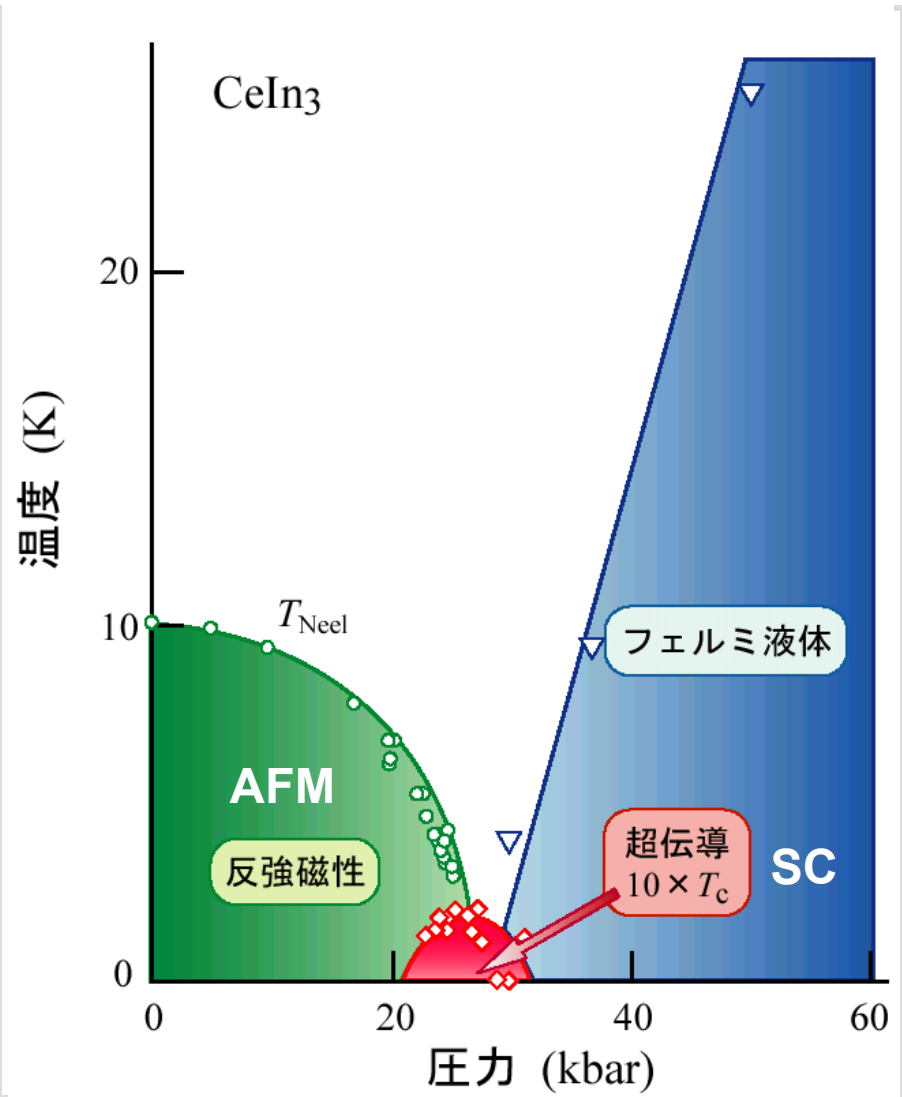
CeIn3
20
10
0
温度 (K)
TNeel
フェルミ液体
AFM
反強磁性
超伝導
10×Tc
SC
0
20
40
60
圧力 (kbar)

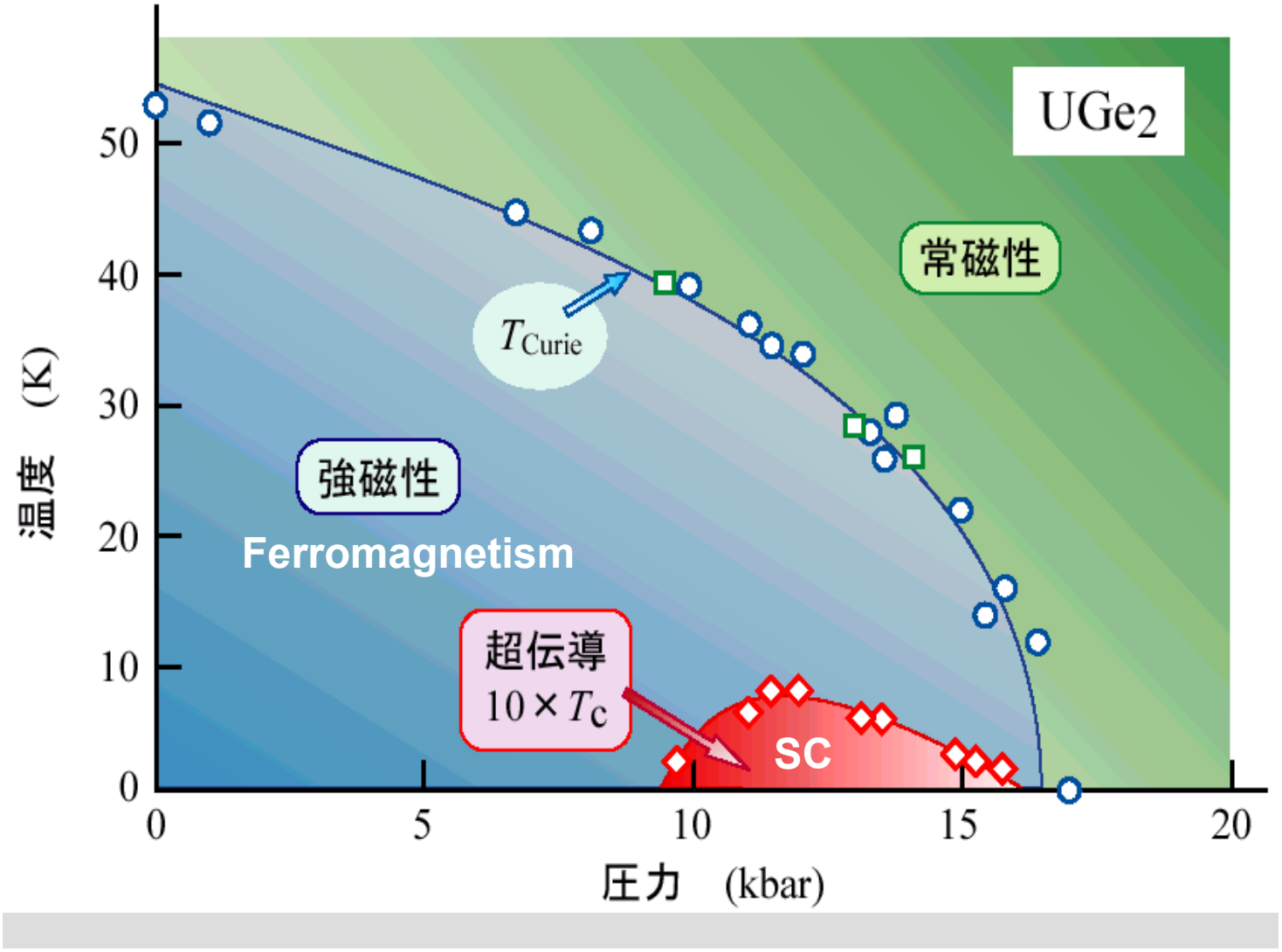

重い電子系における高温超伝導現象

High-T_c phenomenon in Heavy-electron system

Present Status of SC Research Anniversary Since its Discovery

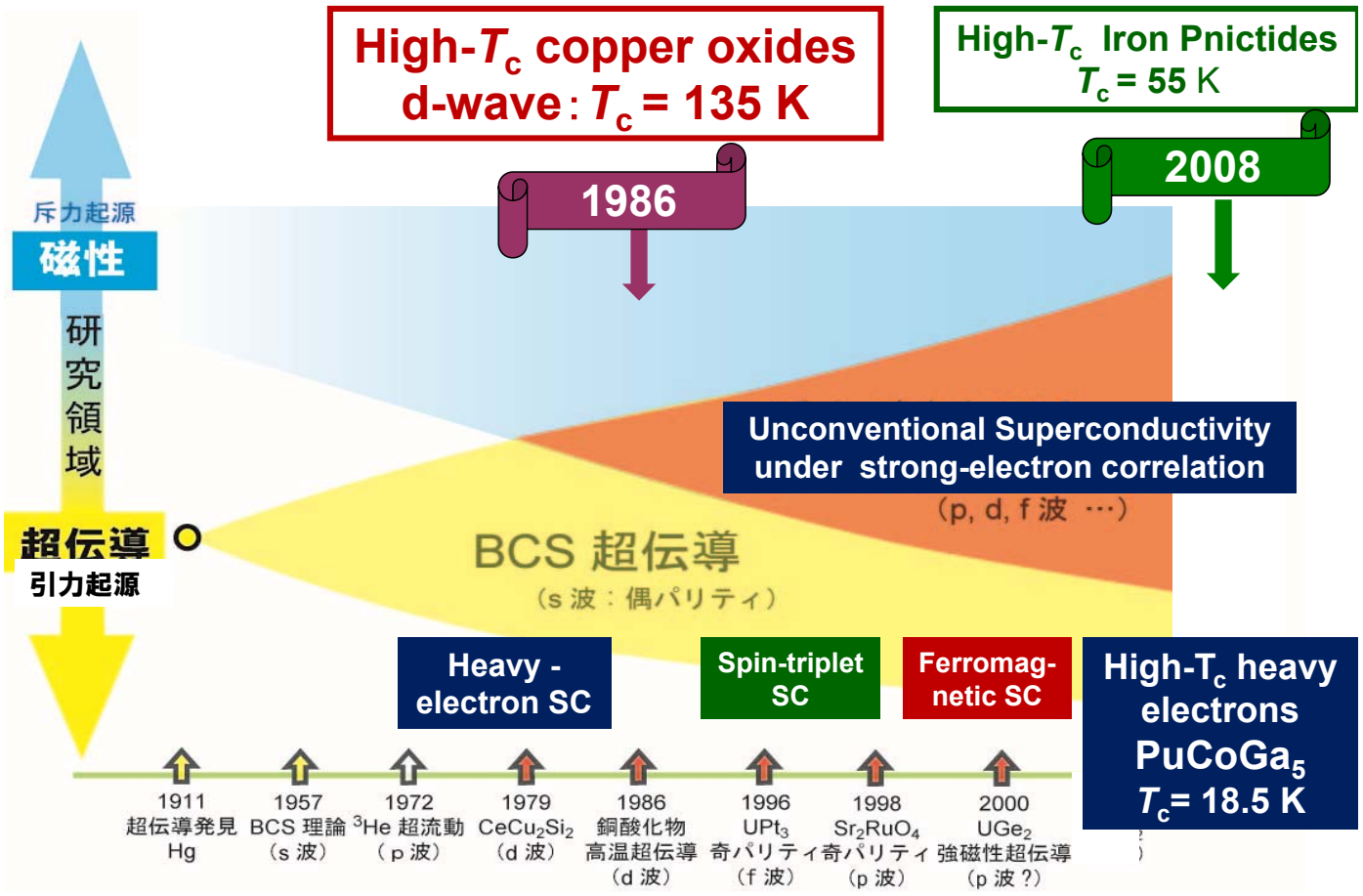

Diversity of Heavy-electron Superconductivity due to Correlation effect

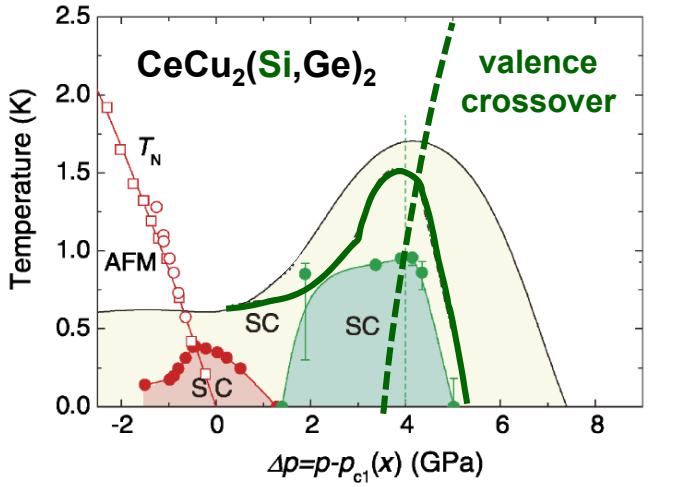

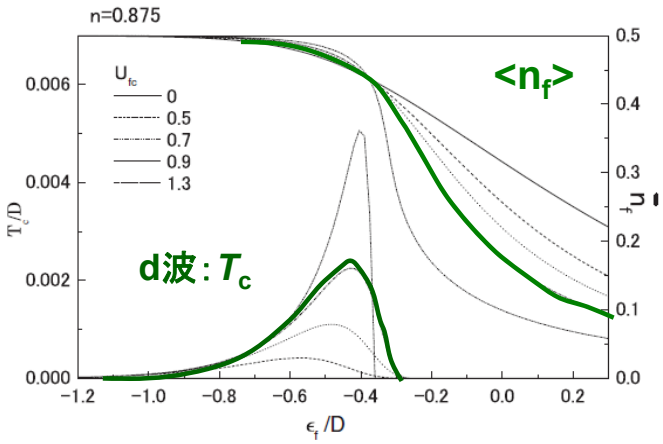

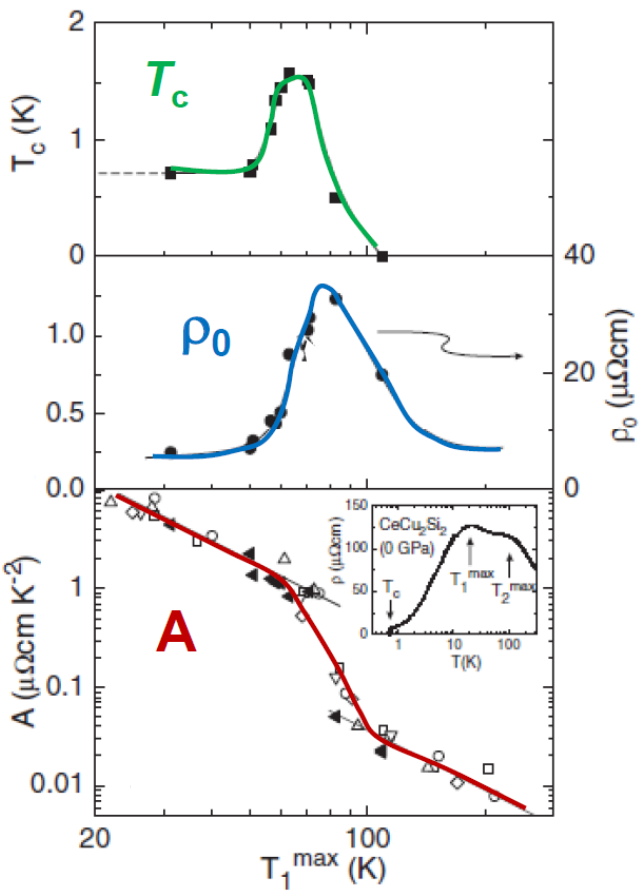

$\rho(T)=\rho_0 + AT^2$

K. Miyake, et al., J. Phys. Soc. Jpn.,76,(2007) 051002.

Valence (electron-transfer) fluctuations induced SC $CeCu_2Si_2$

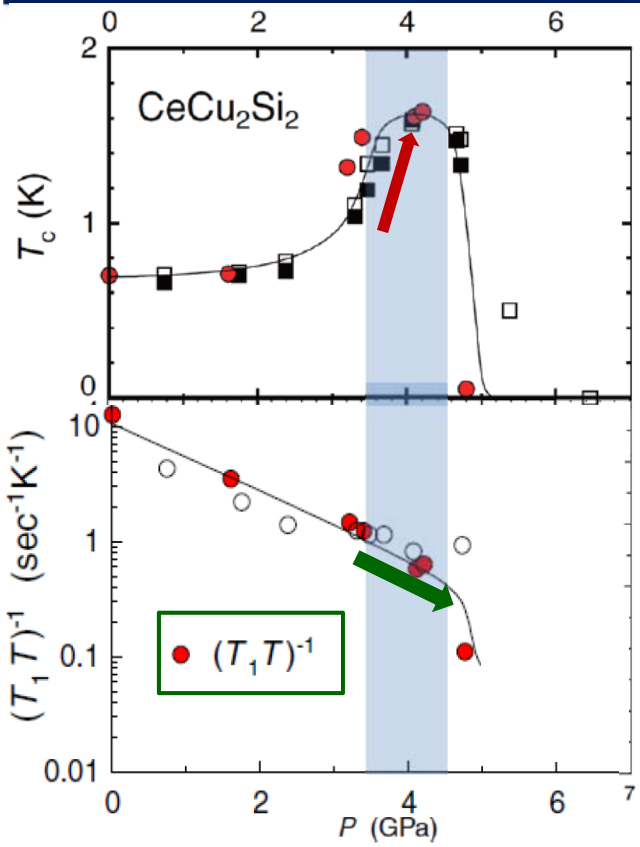

Repulsive interaction U_{fc} between $4f$- and c-electrons plays key-role for valence fluctuations emerging, leading to the onset of a maximum T_c=1.6 K around 4GPa.

A possibility of valence -fluctuation mediated strong-coupling SC.

$\chi''_{loc}(\omega) = \Sigma_q \chi''_q(\omega)$

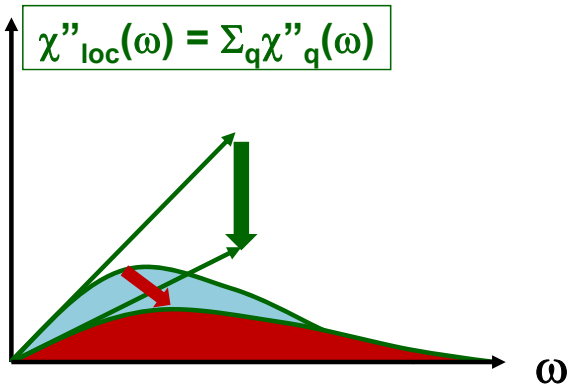

K. Fujiwara et al., JPSJ. 77, 123711(2008).

High-T_c SC in (Ce,Pu)115 compounds

115系	T_c (K)
$CeCoIn_5$	2.3 (d波)
$CeRhIn_5$ (AF: T_N=3.4K)	2.1 (d波) (p=2.1GPa)
$CeIrIn_5$	0.4 (d波)
$PuCoGa_5$	18.5
$PuRhGa_5$	8.6

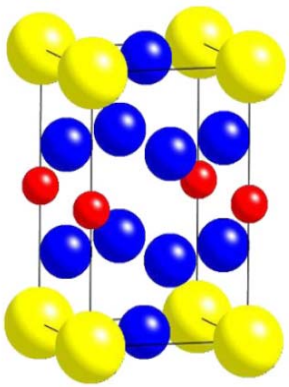

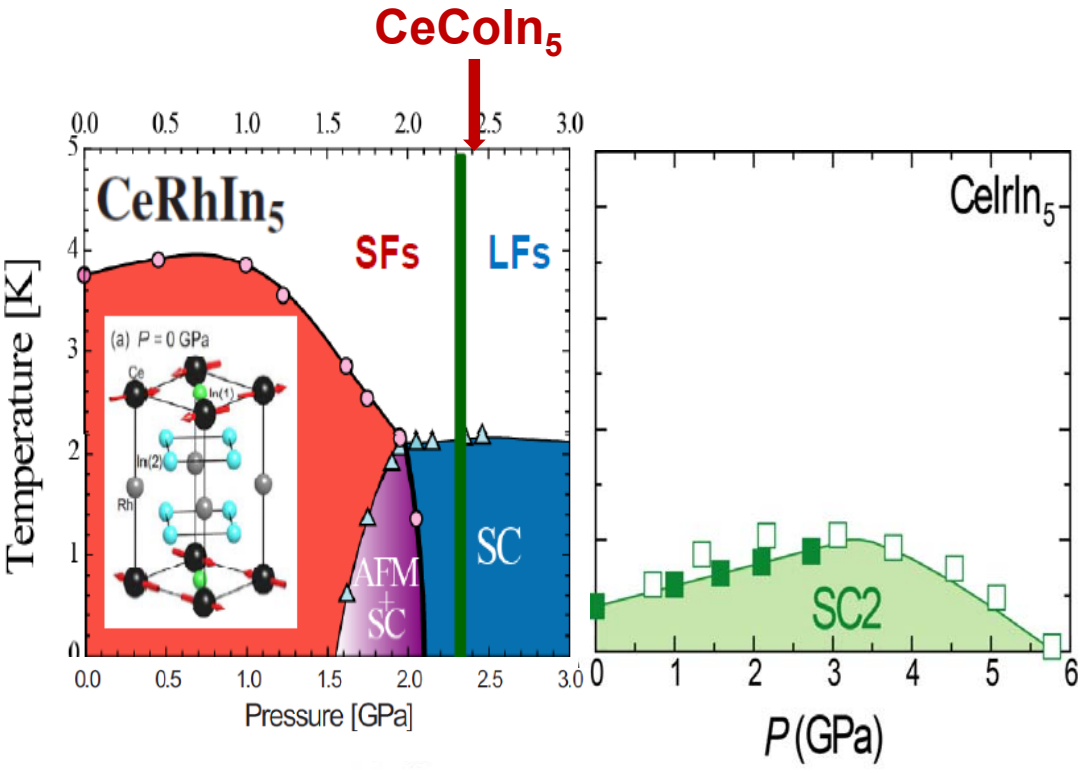

M. Yashima et al ., Phys. Rev. B 79, 214528 (2009).

S. Kawasaki et al., PRL 96, 147001 (2006).
G.-q. Zheng et al., PRL 86, 4664 (2001).
T. Muramatsu et al., Physica (Amsterdam) 388C–389C, 539 (2003).

Characteristics of Magnetic Fluctuations

$(1/T_1T)$ **$CeCoIn_5$: T_c = 2.3 K**

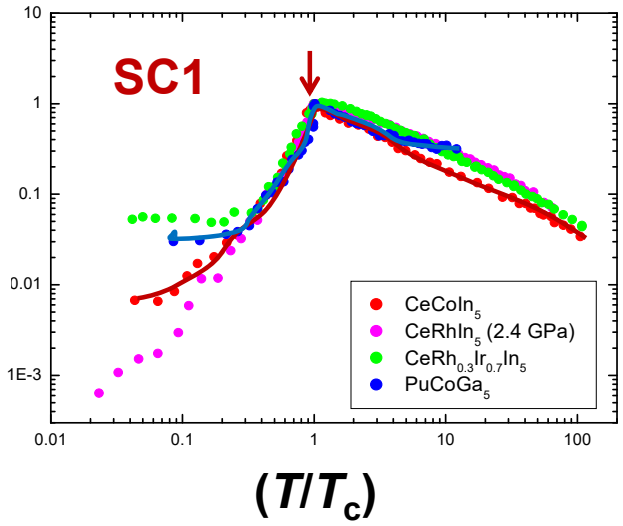

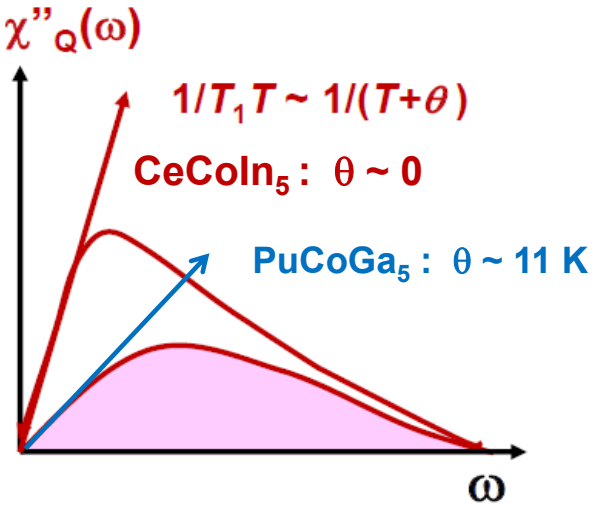

$PuCoGa_5$: T_c =18.5K

J. L. Sarrao et al., Nature 420, (2002) 297.

Magnetic criticality and SC energy gap

$2\Delta_0/k_BT_c$

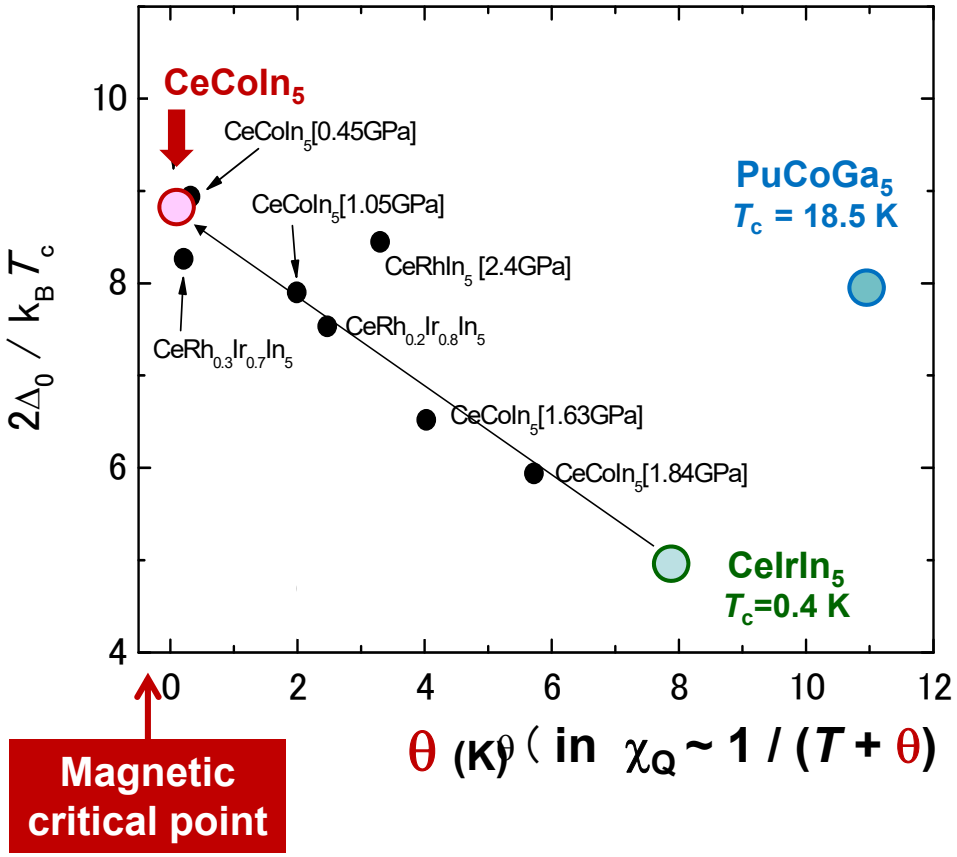

Evolution of electronic state in Ce115 superconductors (pressure effect)

M. Yashima et al., JPSJ 73, 2073 (2004).

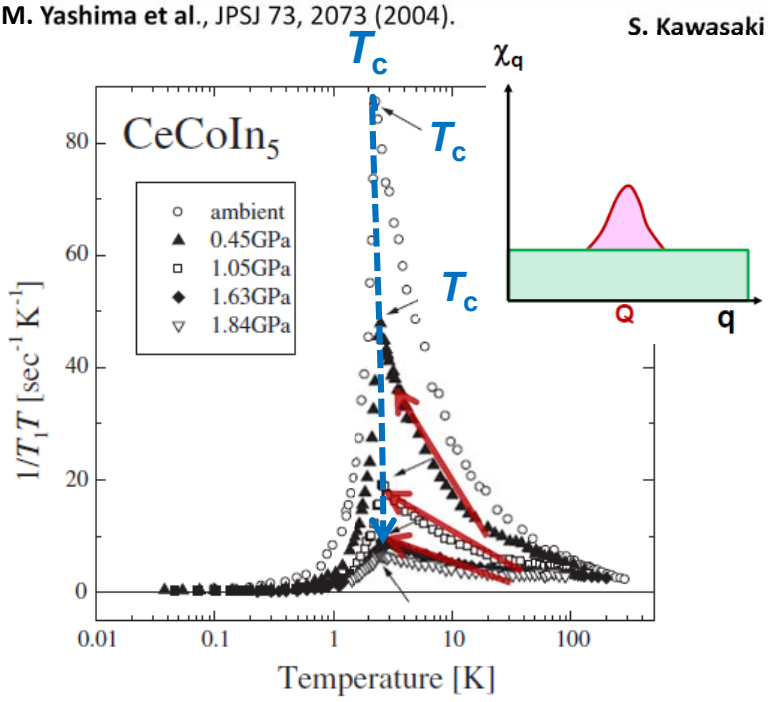

S. Kawasaki et al., PRL 94, 037007 (2005).

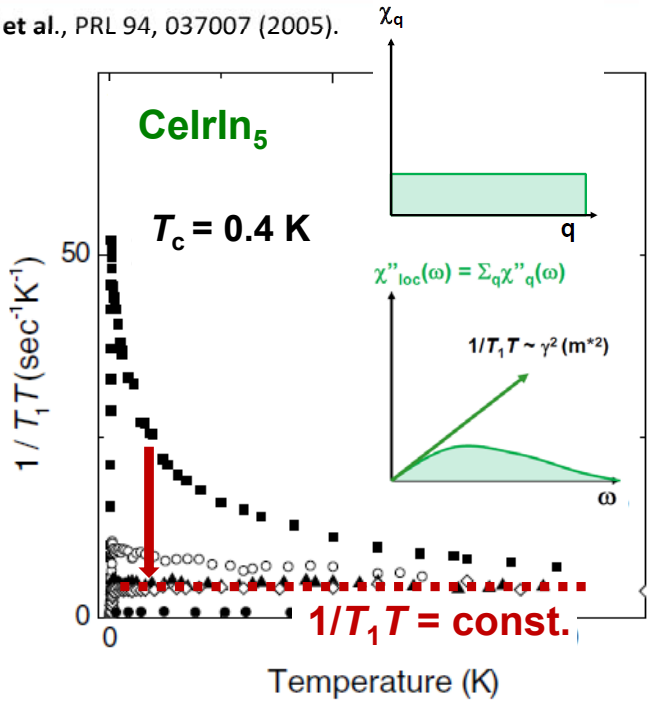

SC1(d_{x2-y2}): $1/T_1T \sim (T+\theta)^n$

SC1: SC induced by spin-fluctuations due to on-site correlation U_{ff}

→ T_c=0.9 K (p=2.7GPa)

SC2 : SC induced by valence-fluctuations due to the neighboring correlation U_{fc}

Almost localized fluctuations-induced SC Characteristics

$(1/T_1T)$ SC2

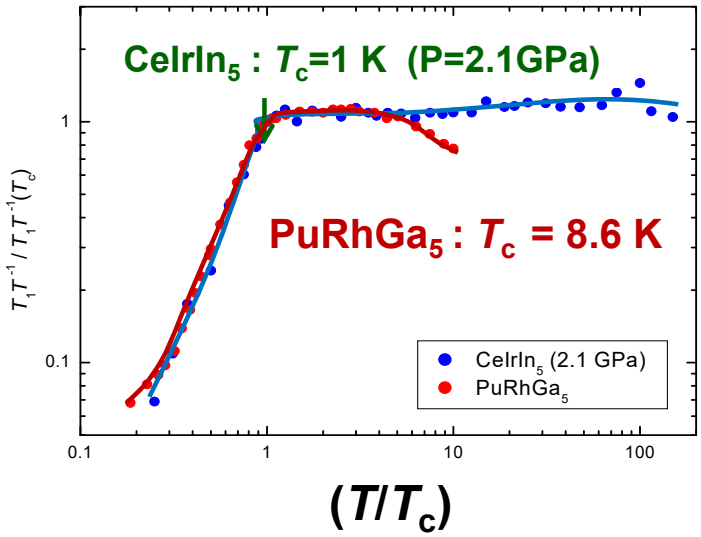

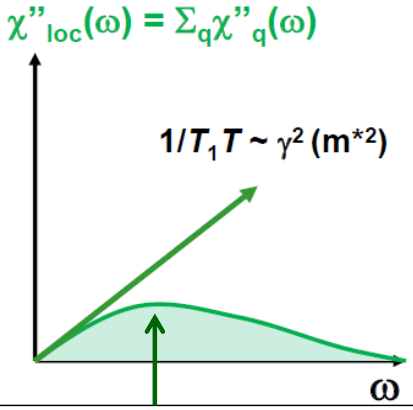

CeIrIn$_5$: Γ_L ~ 80 K to T_c = 1 K

PuRhGa$_5$: Γ_L ~ 600 K to T_c = 8.6 K

Γ_L : (c-f) hybridization, Repulsive interaction among orbits, spin-orbit interaction, muliple fluctuation

PuCoGa$_5$: T_c =18.5 K at Γ_L ~ 600 K and θ ~ 11 K (due to nesting effect？)

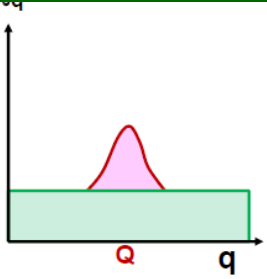

F. Wastin *et al.*, J. Phys.: Condens. Matter **15** (2003) S2279–S2285.

Effective Fermi temperature T^* vs T_c

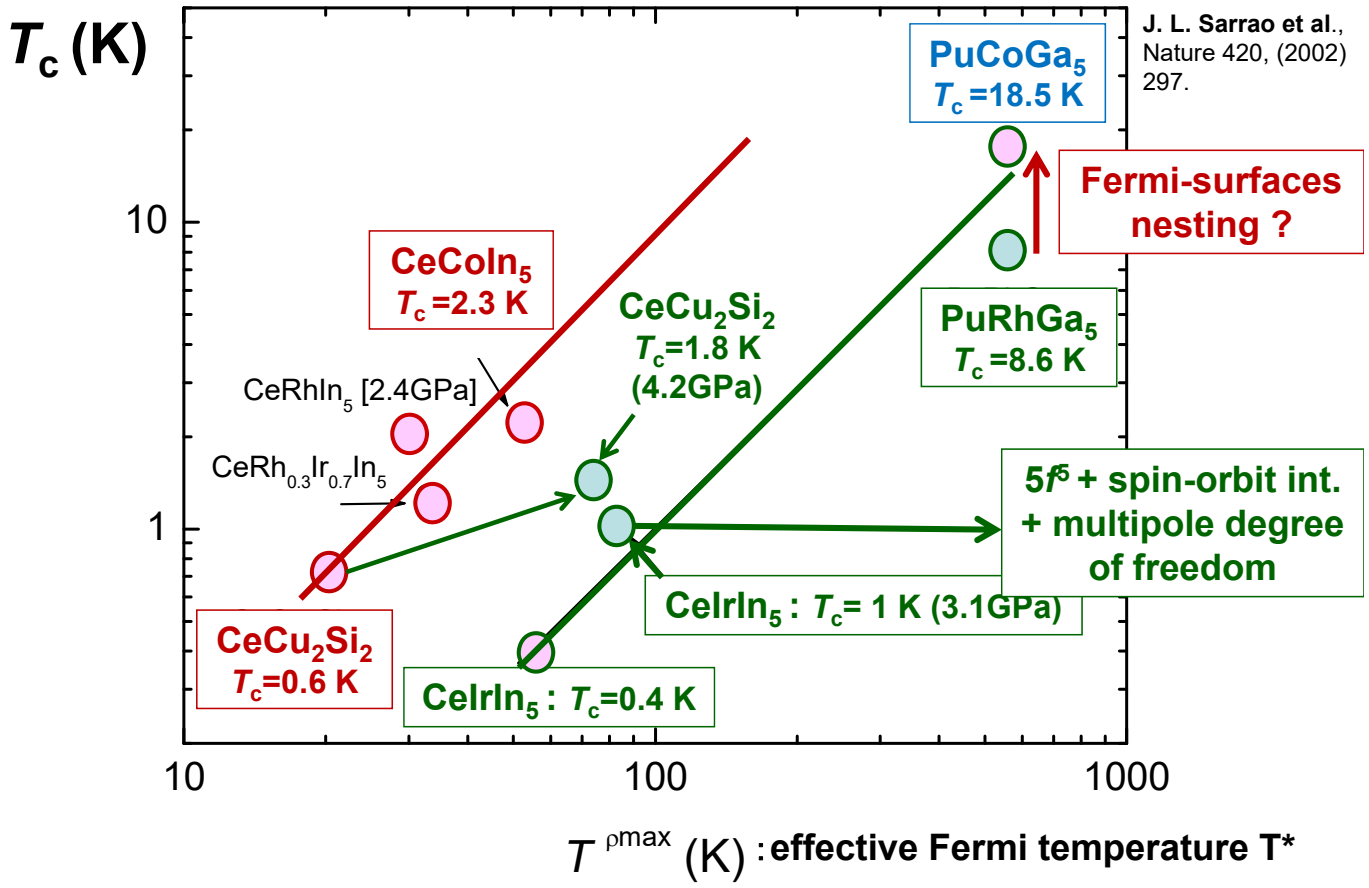

Crystal electric field and Kondo temperature

$$T_K = D_0 \exp(-1/J_0)(D_0/\Delta_1)^2$$

$$J_0 = |J_{ex}\rho(E_F)/N|$$

$$J_{ex} \sim -V_{cf}^2/U$$

K. Yamada, K. Yosida and K. Hanzawa
Comments on the Dense Kondo State
Prog. Theor. Phys. 71, 450-457 (1984)

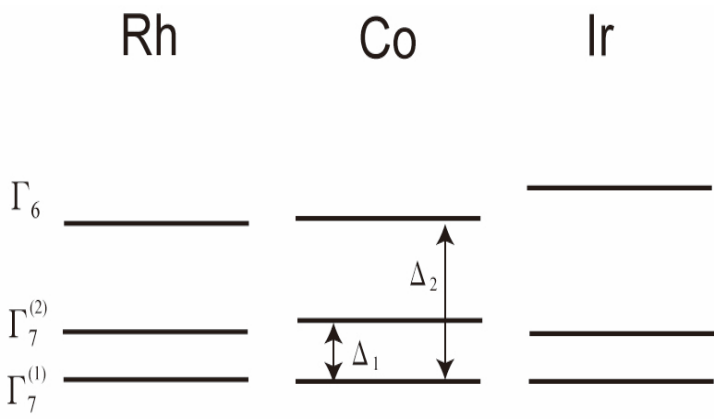

(meV)	$CeCu_2Si_2$	$CeRhIn_5$	$CeCoIn_5$	$CeIrIn_5$
Δ_2	31	24	25	29
Δ_1	12	6.9	8.6	6.7
Quasi-elastic width (~T_K)	1	2.3	6.6	8.7

Inelastic Neutron Scattering: A. D. Christianson *et al*., Phys. Rev. B 70, 134505 (2004)

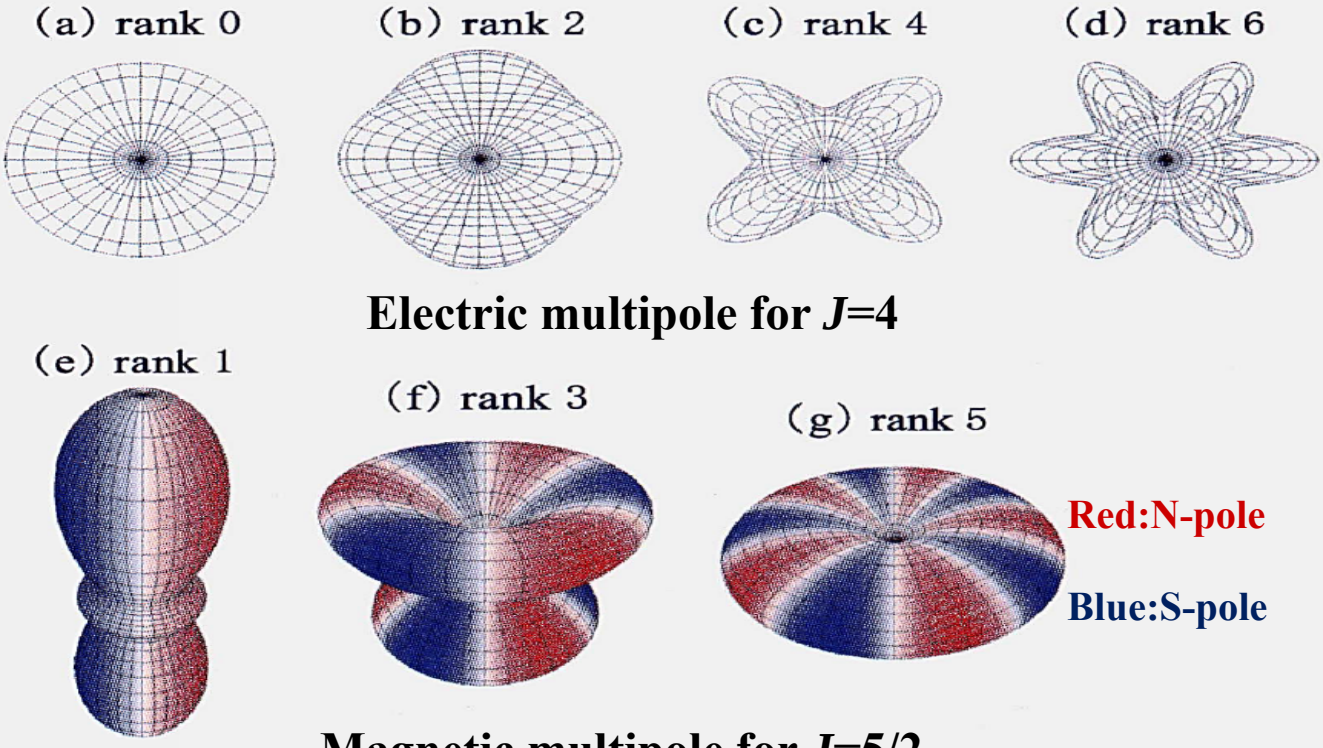

第４図
多極子をともなう波動関数の例.
(a)−(d) 電気多極子（$J=4$），(e)−(g)磁気多極子（$J=5/2$）．波動関数の形状は電荷分布を，カラーマップは磁荷分布（N 極：赤，S 極：青）を表わす．

Overlooking of Heavy-electron Superconductivity

	Heavy electrons systems
Mother compound	Magnetic order, multipole order, quantum critical phenomena
Evolution of phase	Pressure, Chemical substitution
Electronic state	Multi-bands
SC symmetry	*d* -wave, *f* –wave, extend *s*-wave
Pairing interaction	Fluctuations of Magnetic（Spin density), Valence, Multipole, Orbital

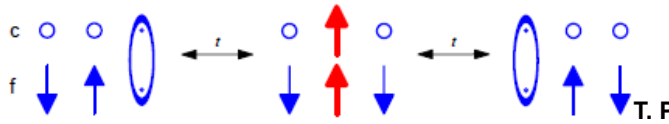

s-wave SC

T. Pruschke etal.,arXiv:1301.5556v1

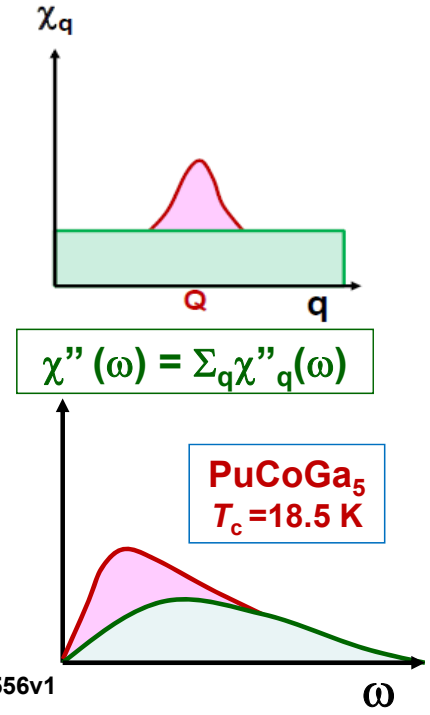

First principle calculation with spin-orbit interaction → Tight binding effective model
→ Introduction of *f*-*f* electrons interaction（U, U', J, J'）
→ dealing with magnetic order and multipole order under the multiband including heavy and light mass Fermi surfaces,
→ understanding a possible onset of SC mediated by either wave number dependent fluctuations and almost localized fluctuations

Reaction mechanisms of the Mn_4CaO_5 cluster of photosystem II in PLANT

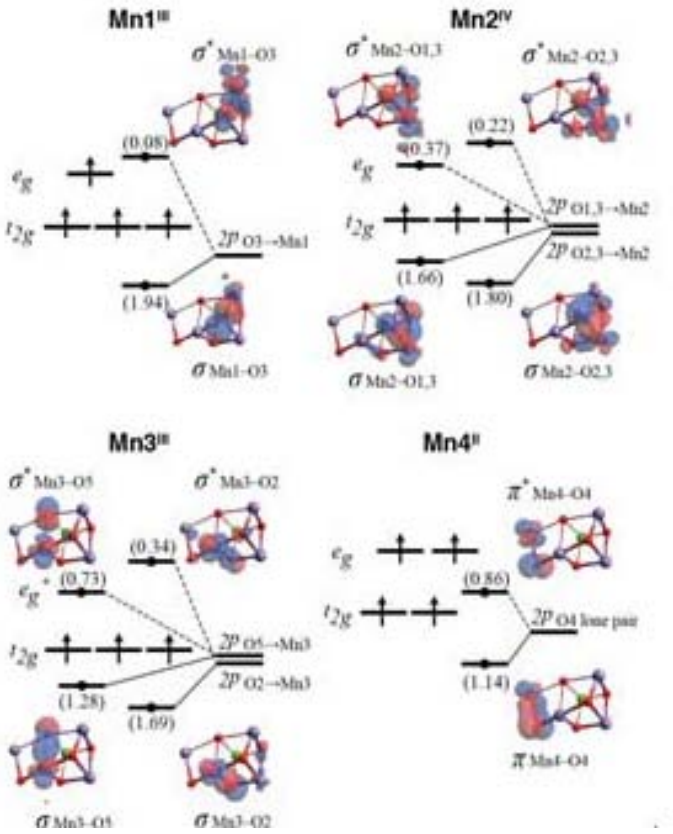

Development of efficiency or the figure of merit in the reaction process of photo-catalysis is the intensive research subject of matter science

Honda-Fujishima effect : visible light can decompose water into oxygen and hydrogen in the electrochemical cell in which TiO_2 electrode is connected with a platinum electrode.

Unfortunately, the industrial mass-product is not available yet. It is highly desired to create hydrogen as clear energy source by means of this photo-catalysis function. We may call this TiO_2 as an uncorrelated photo-catalysis matter.

The stabilization of surface-associated intermediate Mn^{3+} species is brought about by the formation of N–Mn bonds in which the inorganic Mn-oxide hybridizes with the coordination of organic amine. Then, the charge disproportionation is inhibited to lower the overpotential for water oxidation by MnO_2.

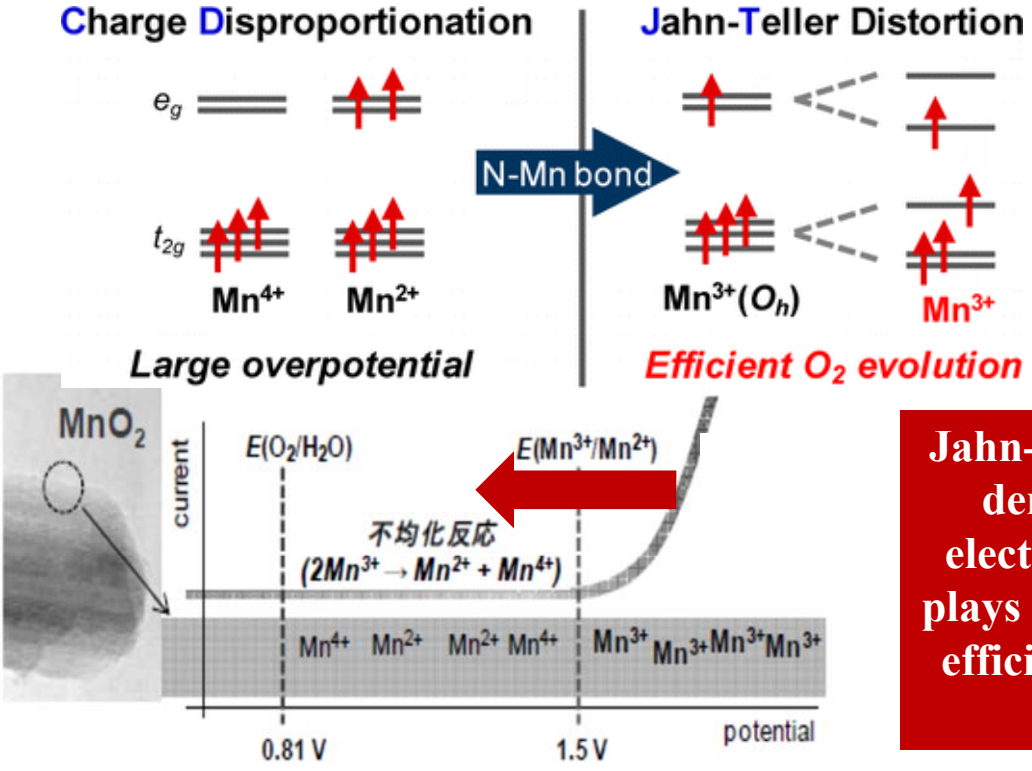

Jahn-Teller Distortion derived local 3d-electrons correlation plays a key-role for the efficient O_2 evolution from H_2O

Summary

The many-body electron correlation in condensed matter is a key-ingredient for creating the emergent phases and functional materials.

The local electron correlation may be relevant with the emergent functions in non-periodic complex systems such as metal catalyst, photo-catalysis reaction in plant and even biological matter with transition-metal elements.